ChemComm

FEATURE ARTICLE

View Article Online
View Journal

Cite this: DOI: 10.1039/d5cc07008b

Polymer-tethered glycosylated gold nanoparticles as versatile tools for bio-sensing

Sarah-Jane Richards *[a] and Matthew I. Gibson *[ab]

Received 9th December 2025,
Accepted 14th January 2026

DOI: 10.1039/d5cc07008b

rsc.li/chemcomm

Glycans direct many biological recognition and signalling processes, spanning basic cell biology to diagnostics and therapy. Multivalent presentation of glycans is well established to increase avidity (but not always selectivity) and hence glycosylated (nano)materials have emerged as versatile scaffolds to probe glycobiological processes and for application in biomedicine. In this Feature article we review our laboratory's contributions to the development of polymer-tethered glycosylated gold nanoparticles. This approach exploits the steric stability of the polymer coating, ease of glycan capture and the plasmonic signal-generation of the gold core. The article covers the synthetic rationale for the polymeric tether, glycan capture modalities and application to screen (un)natural glycans binding patterns and translation into point-of-care lateral flow glyco-diagnostics and solution-phase colourimetric biosensors. We also suggest areas for future development and comparison to related systems.

1. Introduction

Carbohydrates (glycans) are one of the four major classes of biological macromolecules, in addition to nucleic acids, proteins and lipids.[1] These complex macromolecules fulfil a variety of tasks ranging from structural and metabolic function to regulating development, cell signalling, cell adhesion, and host–pathogen interactions. It has been reported that more than 50% of the human proteome is glycosylated and that 2% of the human genome is dedicated to glycosylation processes.[2] Lectins are the primary carbohydrate-binding proteins (other than enzymes and antibodies) that act as the 'readers' of glycans. The binding affinity of a carbohydrate to its lectin

[a] Department of Chemistry, University of Manchester, Oxford Road, Manchester, M13 9PL, UK. E-mail: matt.gibson@manchester.ac.uk, sarah-jane.richards@manchester.ac.uk
[b] Manchester Institute of Biotechnology, University of Manchester, 131 Princess Street, Manchester, M1 7DN, UK

Sarah-Jane Richards

Dr Sarah-Jane Richards is a Research Fellow at the University of Manchester. She obtained her PhD from the University of Warwick, where she focused on the design and synthesis of glycosylated nanomaterials. Her research combines polymers and nanoparticles to interrogate protein–carbohydrate interactions, providing insights into biological recognition processes. By integrating synthetic chemistry with nanotechnology, she aims to design innovative platforms for studying complex biomolecular systems and translating these findings into practical applications. A key focus of her work is the development of rapid point-of-care diagnostic technologies, leveraging molecular recognition to enable early detection and improved healthcare solutions.

Matthew I. Gibson

Professor Matthew Gibson holds a Chair in Sustainable Biomaterials at the University of Manchester, UK. After a PhD at the University of Durham, and a post-doc at EPFL (Switzerland), he established his group at the University of Warwick (2009–2023). His multidisciplinary research group develops new materials to address challenges in Biotechnology, Healthcare and Sustainability. He has held ERC Starter and Consolidator Grants and undertaken technology transfer including as a Royal Society Industry Fellow and cofounding spin out(s). Matt has been awarded prizes including the Corday Morgan, McBain, Dextra and MacroGroup Young Researcher's medals and an RSC Horizon Prize.

target is typically weak (K_a = 10^3–10^6 M^{-1}), compared to antibody-antigen interactions which are typically greater than 10^9 M^{-1}.[3] Nature circumvents this limitation through the "cluster-glycoside effect", where multiple copies of the same glycan are presented on a cell surface, dramatically enhancing overall binding strength *via* multivalent interactions.[3–5] This avidity gain arises from cooperative binding, reduced dissociation rates, and increased local concentration of ligands at the interface.[6] Multivalency is a fundamental principle in biological recognition, underpinning processes such as viral adhesion, immune signalling, and cell–cell communication. It enables selectivity and robustness in systems where individual interactions are inherently weak, inspiring synthetic strategies for inhibitors, vaccines, and diagnostics.[7,8] Glycosidases and glycosyltransferases act as the 'writers/erasers'[9] of glycans and their complex interplay based on their spatiotemporal distribution dictates the formation and presentation of glycans.[10] It is also important to highlight there are anti-glycan antibodies.[11,12]

The wide range of functions carried out by carbohydrates is reflected in their structural diversity. Glycan structural and chemical diversity is determined by the specific combination of selected elements from a set of monosaccharide building blocks: the different glycosidic linkages used to link these monosaccharides, the stereochemical configuration of the glycosidic bonds, branching and site-specific modifications (such as sulphation and phosphorylation) lead to the complexity of the glycome,[13] making them the most structurally diverse biomacromolecule. This heterogeneity makes isolation of pure samples, and in sufficient amounts, from biological sources challenging in many cases.[14] Several techniques are typically required to be used in parallel such as high-performance liquid chromatography (HPLC), mass spectroscopy (MS), nuclear magnetic resonance (NMR) and array technologies (glycan and lectin arrays).[2,15–22] In contrast, a single technique can be used to interrogate RNA, DNA or proteins including gene mutation, over-expression, and silencing which is challenging in glycobiology as glycans are not template-encoded. Fluorescent labelling can be genetically included to tag proteins for visualisation to study localisation.[17] Protease enzymes are available to digest proteins and assignment of the protein sequence can be carried out by MS. A difficulty of MS for glycan characterisation is the discrimination of several structural isomers, such as enantiomers (*e.g.* D/L-glucose), diastereoisomers (*e.g.* glucose/mannose), anomers (α/β), and linkages and branching (*e.g.* 1–4/1–6).[4] Progress in glycoscience has been hindered by the lack of analytical methods that can accurately map glycan structures, particularly distinguishing α/β anomeric linkages in oligosaccharides. Flitsch and co-workers have demonstrated that the anomeric configuration is preserved after gas-phase glycosidic bond fragmentation during tandem mass spectrometry (MS^2). By integrating MS^2 with ion mobility spectrometry (IM-MS^2), differentiation of α- and β-linkages in natural, underivatised carbohydrates can be achieved. This was validated on oligosaccharide standards and applied to sequencing of plant glycoconjugates, revealing that anomeric signatures persist in fragments from larger glycans.[23–25] For nucleic acids sequencing and microarray technologies can be used alongside amplification which are not possible for carbohydrates[26] adding to the challenge.

Carbohydrate arrays (glycoarrays) have emerged as the primary high-throughput tool for studying carbohydrate/lectin binding (Fig. 1).[11] Glycans can be covalently or non-covalently linked to a solid support surface (*e.g.* alkyne-azide 'click', thiolene 'click', activated esters) which can require non-trivial multistep, protection and deprotection sequences. The non-covalent attachment of glycans has been performed by Feizi *et al.*,[27] using neoglycolipids (NGL) that adsorb onto hydrophobic surfaces, but retain some mobility to form clusters for optimal protein binding, as occurs in cell membranes. As an example,

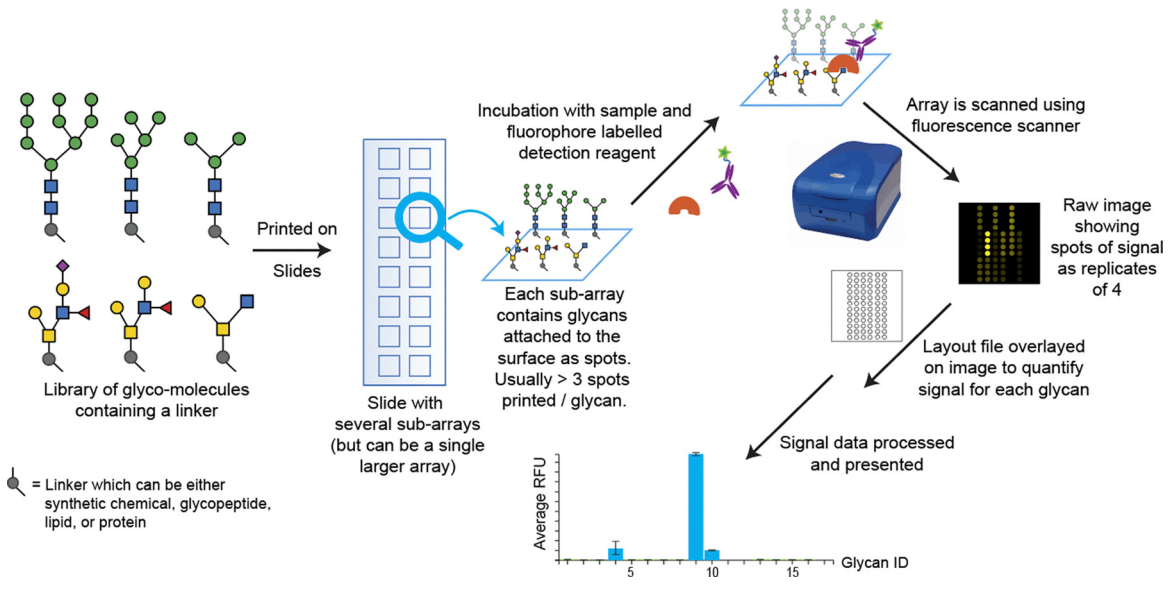

Fig. 1 Overview of construction and analysis of glycoarrays, Reproduced from Heimburg-Molinaro *et al.* ref. 40 with permission from Elsevier, copyright 2024.

this technology was used to interrogate human and swine influenza strains against a panel of 86 glycans (80 sialylated and 6 neutral (control)). A clear difference in receptor-binding was observed between pandemic H1N1 viruses (Cal/09, Ham/09) and the seasonal virus Mem/96. Cal/09 and Ham/09 bound broadly to α2-6-linked sialyl sequences regardless of backbone type or length, and to many α2-3-linked sequences. In contrast, Mem/96 bound exclusively to α2-6-linked sequences.[28] More recently solution phase arrays based on chemically glycosylated phages have emerged, enabling genetic encoding and high-throughput screening.[29]

Another powerful tool to probe intracellular glycan function is metabolic oligosaccharide engineering (MOE) which uses unnatural glycans to hijack a cell's biosynthetic machinery, to allow unnatural (and bio-orthogonal[30,31]) glycans to be integrated into glycoconjugates spanning the cell surface,[32–34] glycoproteins[35] and glycoRNA.[36–38] The majority of these are secreted or cell surface glycoproteins, but some are found inside the cell.[39] Metabolic oligosaccharide engineering has been applied to myriad problems in glycobiology; to disrupt glycan biosynthesis, chemically modify cell surfaces,[32] probe metabolic flux inside cells, and for proteomics analysis of glycosylation.

The above summary showed examples of advances in glycomics which are generating new opportunities to exploit glycan binding processes in biosensing and diagnostics. For example, many respiratory pathogens (including SARS-CoV, SARS-CoV-2, influenza) and bacterial pathogens (such as uropathogenic *E.coli*) target and anchor glycans as key stages in their infection cycle and many cancers are associated with glycosylation changes.[41,42] New tools, including those suitable for point of care diagnostics, are needed to intercept, detect and diagnose these crucial pathways and processes which are discussed in the following section.[43–45]

1.1. Gold nanoparticles as biosensors

Gold nanoparticles (AuNPs) exhibit characteristic optical properties that are dependent on surface plasmon resonance (SPR), which arises due to the collective oscillation of the conduction-band electrons. The maximum wavelength and shape of the local surface plasmon resonance (LSPR) are determined by the particle size and shape. AuNPs have extremely high extinction coefficients, which are three to five orders of magnitude greater than those of traditional molecular dyes and is stronger than other metal plasmonic nanoparticles. The SPR band intensity and wavelength depends on the factors affecting the electron charge density on the particle surface such as the metal type, particle size, shape, structure, composition and the dielectric constant of the surrounding medium, as theoretically described by Mie theory.[46] As a result of the above, spherical AuNPs between 10 nm and 80 nm appear red in colour (due to absorption of blue-green portion of the spectrum ~450 nm). As the interparticle distance decreases to less than that of the particle diameter, coupling and dipole–dipole interactions between the plasmons of neighbouring particles result in a broadening and a shift to longer wavelengths of the surface plasmon absorption band, resulting in the AuNPs appearing blue. It is this colourimetric aggregation that is exploited for the use in bioassays which can be detected spectrophotometrically, or visually by eye or with cameras.[47]

Colourimetric assays for investigating biomolecular interactions using AuNPs functionalised with biomolecules such as proteins,[48,49] peptides,[50,51] antibodies,[52–54] and DNA,[55,56] have been developed based on inducing particle aggregation (Fig. 2A/B). The detection of bacterial DNA using AuNPs originated in the pioneering work of Mirkin *et al.*[55] who demonstrated that as little as 10 fmol of an oligonucleotide analyte could be detected by exploiting the aggregation phenomenon of AuNPs.

Lateral-flow diagnostics (LFD) are another sensing modality which deploy gold nanoparticles, most famously the home-pregnancy test,[57] which make use of the high extinction coefficient (strong colour) of the gold nanoparticles. Traditional LFDs use antibodies (lateral flow *immuno* diagnostics) as the detection units immobilised to both the stationary phase (*e.g.*, nitrocellulose paper) and the mobile phase (AuNPs), forming a "sandwich" with the analyte in the middle, giving a red line

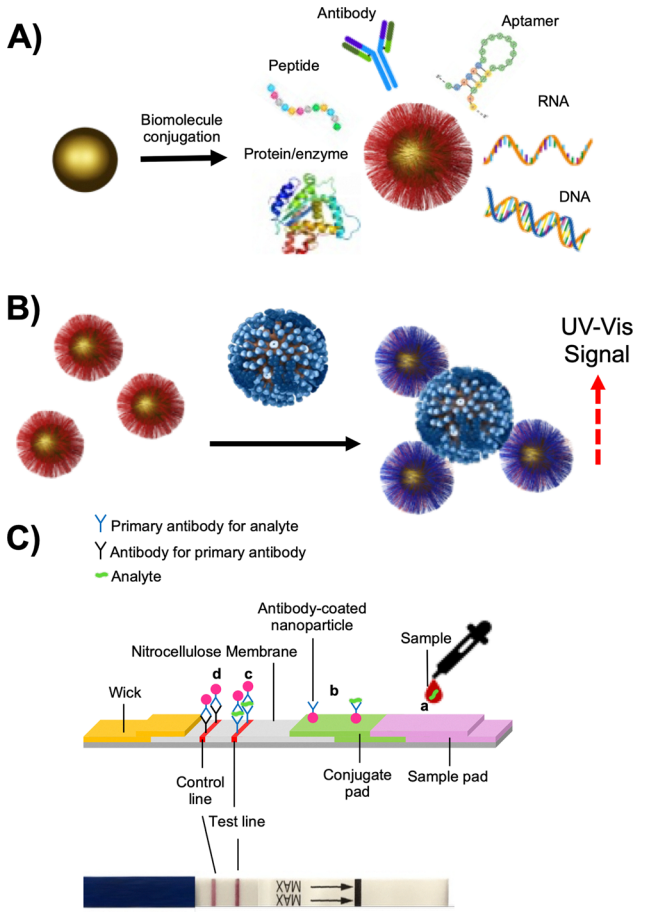

Fig. 2 Gold nanoparticles in biosensing. (A) General procedure for functionalising AuNPs with biomolecules; (B) principle of aggregation-induced colour change of AuNPs in response to a stimulus; (C) AuNP in lateral flow diagnostics.

due to concentration of the AuNPs (Fig. 2C). LFDs are typically low cost and require little or no clinical infrastructure or training to use. *Immuno*-LFDs tend to have lower sensitivity (some false negatives) but high selectivity (few false positives). The cost-effectiveness and clinical usefulness of these inexpensive devices has been demonstrated by various studies of malaria rapid diagnostic tests[58,59] in the diagnosis of cutaneous leishmaniasis[60] and were found to compare well to the more expensive RT-PCR for Ebola diagnosis.[61] In addition to antibodies, other recognition unit such as nucleic acids,[62] glycans, and lectins[63] could be used, provided they have suitable characteristics (affinity, selectivity, specificity). During the COVID-19 pandemic LFDs were extensively explored due to their low cost and rapid turnaround time which could enable regular mass testing of large populations.[64] This could find asymptomatic individuals spreading the virus, who would not be identified by a symptomatic RT-PCR testing pathway.[65–67] The first LFDs for the COVID-19 pandemic were designed to detect antibodies in patient blood samples produced in response to SARS-CoV-2 infections to repot prior infections.[68–70] Antigen LFDs, in contrast, were designed to diagnose the presence of the virus *i.e.*, an active infection. Several antigen lateral-flow tests, by late 2020, had passed Phase 3 testing in the United Kingdom,[71] gained WHO "Emergency Use Listing" approval,[72] or had emergency approval granted by The United States Food & Drug Administration. These devices all utilise antibodies as detection/capture units. A university-based validation testing between LFDs and PCR confirmed that LFDs cannot detect lower viral loads but were estimated to be capable of identifying up to 85% of infections in the cohort trialed[67] showing their potential for frequent, low-cost testing when deployed appropriately.

Considering the above applications of gold nanoparticles in biosensing/diagnostics and the critical role played by glycans in cellular recognition processes, our team (and others) have been developing the tools and applications for integrating glycans onto gold nanoparticle surfaces to re-purpose these for glycobiology. This Feature Article focusses on reviewing our laboratory's development of polymer-tethered glycans, using the polymers as adapters to allow capture of the glycans and immobilisation onto the gold and to provide steric (colloidal) stabilisation. We review the synthetic principles behind this platform, the integration into tools and then the deployment as new arrays, diagnostics and biosensors, using native and unnatural glycans.

2. Polymer-tethered glycosylated gold nanoparticles

Glycosylated gold nanoparticles that change colour due to lectin-mediated aggregation are well known for their use as biosensors, but we and others identified a key challenge associated with direct immobilisation of glycans onto AuNPs: that the glycans provided insufficient colloidal stability in buffer or complex media, meaning aggregation (and hence false positives) was not always due to 'binding', but due to colloidal instability. To exemplify this problem we immobilised 1-thio-1-deoxy-glucose onto AuNPs using the one-pot method of Watanabe *et al.*[73] Concanavalin A (Con A: a lectin with affinity to α-mannose/glucose) binding was studied by UV-Vis spectroscopy

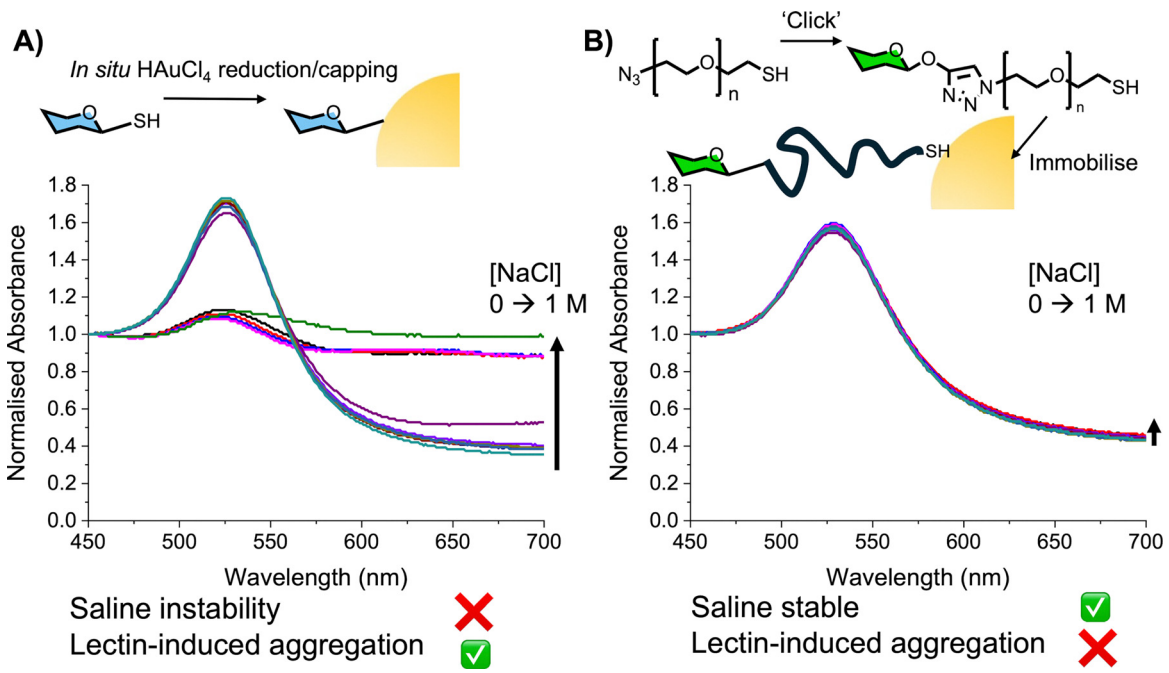

Fig. 3 Delicate balance of nanoparticle colloidal stability to enable aggregation-induced outputs, shown by UV-vis analysis of nanoparticle aggregation. (A) AuNPs with a glucose directly immobilised to the surface readily aggregate in saline, but also responses rapidly to lectins; (B) PEG-linked glycosylated AuNPs are sterically stabilised against saline but show slow lectin binding response.

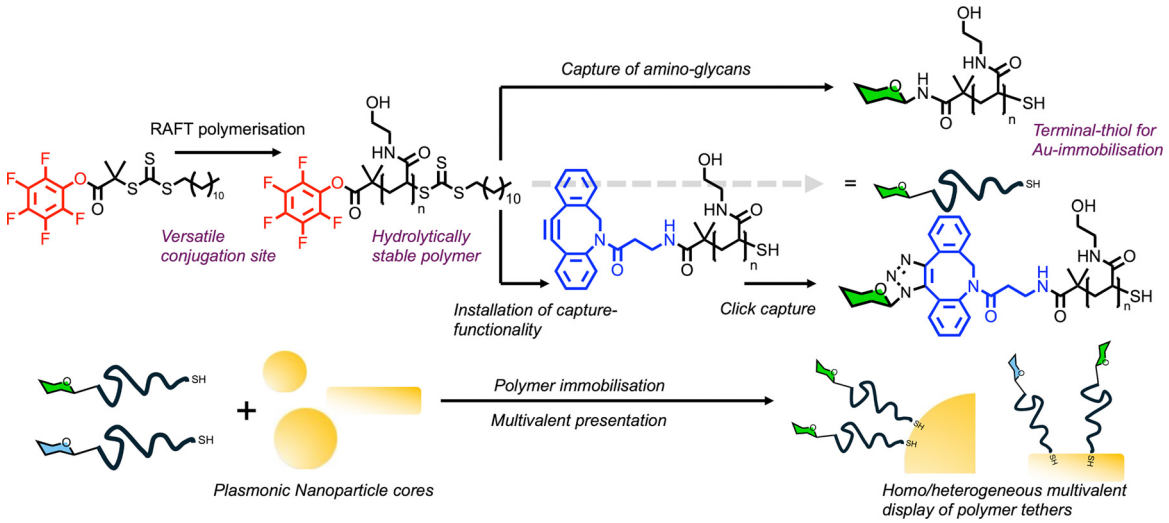

Fig. 4 Summary of the use of RAFT polymerisation to obtain heterotelechelic poly(hydroxyethyl acrylamide) tethers suitable for glycan capture and immobilisation onto gold nanostructures.

showing that larger AuNPs gave response at lower concentration compared to smaller, showing the detection principle. However, a very low salt buffer had to be used due to the instability of particles which readily aggregated to give false-positive 'binding' responses (Fig. 3B). To overcome this, a PEG (poly(ethylene glycol)) tether was introduced as a steric stabiliser to improve the saline stability. Due to the stabilisation, the signal generation was both slower and weaker, taking 2 hours to give equivalent response as 15 minutes with directly glycosylated AuNPs (Fig. 3B). These first experiments highlighted the crucial role of the steric stabiliser, which has to balance stabilisation with allowing aggregation (the output) to still occur.[74] This balance is shown in many studies using PEG as a tether, including work from Field and coworkers.[75–77] In related work, Miura and co-workers have made glycopolymers (with glycan side-chains, not end groups) for immobilisation onto gold nanoparticles for probing lectin-binding.[78,79] Parry *et al.* used a similar strategy to synthesise glycoparticles for immunisation.[80]

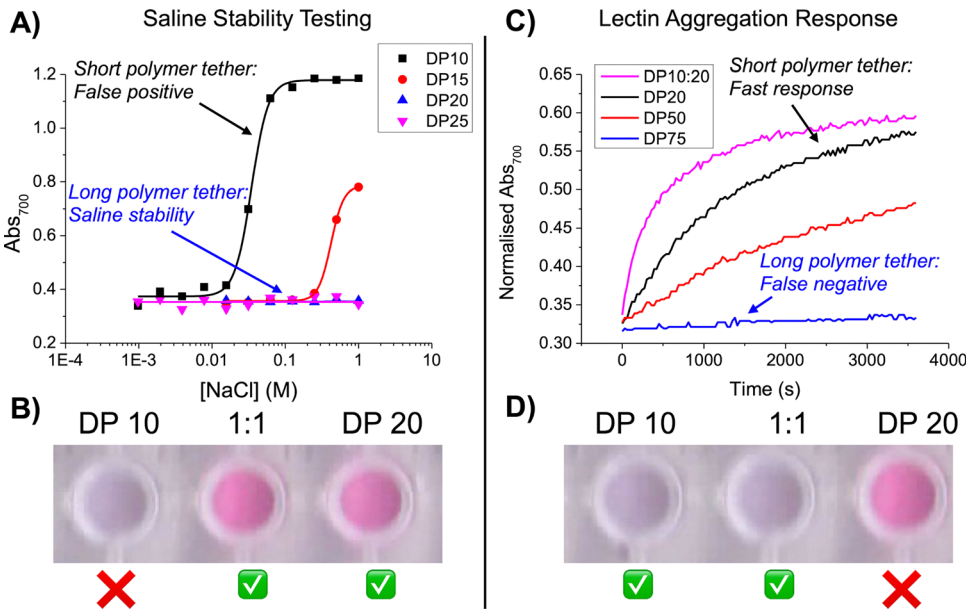

Fig. 5 Impact of PHEA degree of polymerisation on the performance of polymer-tethered glycosylated gold nanoparticles. (A) Aggregation (from UV-vis) as a function of PHEA DP on gold nanoparticles verses a NaCl gradient; (B) photographs showing the colour change in PBS; (C) Con A-induced aggregation kinetics of $ManNH_2$-termintated polymer coated 60 nm AuNPs as a function of PHEA DP in response to 1 mg mL^{-1} Con A; (D) photographs showing Con A-induced aggregation of $ManNH_2$-terminated polymer coated 60 nm AuNPs. Reproduced from ref. 82 with permission from American Chemical Society, copyright 2014.

2.1. PEG alternatives from RAFT polymerisation

Whilst PEG is a useful linker, there are limits to what is commercially available in terms of hetero-bi-functionality and molecular weights, and in our hands some commercial PEGs can contain chain-end defects, limiting application. Therefore, we considered the use of reversible-addition fragmentation chain transfer (RAFT) polymerisation as it is a versatile controlled radical polymerisation (CRP) technique, applicable to a wide range of monomers.[81] The benefits of RAFT have been widely explored, but our interest lay in:

(1) The ability to fine-tune polymer length to optimise stability of coated AuNPs[82]

(2) Incorporation of (latent) functionality at the α-chain end (*e.g.* for glycan capture)

(3) The ω-thio-carbonyl-thio end-groups, which in the presence of a reducing agent, or nucleophiles, cleaves to reveal a thiol-end group for subsequent AuNP immobilisation.

We designed a telechelic polymer system, with a conjugatable pentafluorophenyl ester at the α terminus for facile immobilisation of amino-glycans (or other functions) and a masked thiol (RAFT agent) at the ω-terminus for gold surface immobilisation. Poly(*N*-hydroxyethylacrylamide) (PHEA) was chosen as the polymer of choice for several reasons (Fig. 4). Firstly, it is highly water soluble, but also in organic media, unlocking a variety of chemistries. PHEA is sterically smaller than oligo(ethyleneglycol)(meth)acrylates (OEG(M)As) which we hypothesised would impact grafting density, as previous shown when "grafting to" flat gold surfaces.[83] PHEA does not show lower critical solution temperature, unlike some other water-soluble monomers like OEG(M)As, which would complicate assay performance.[84] Finally, the amide (rather than ester) linkage is more stable, preventing thiol back-biting which has been reported for (meth)acrylates.[85] The use of PFP-terminated polymers, rather than using glycosylated RAFT agents, ensures that all the polymers in a series have the same initial chain length distribution and therefore reduce the variability between particle types (when varying particles size or glycan for example).

Using a panel of PHEAs of different molecular weights (degree of polymerisation, DP = 10–75) it was observed that polymers of DP <15 on AuNPs of 60 nm were unstable at raised [NaCl] (>0.2 M, which is close to physiological (0.137 M)), making them unsuitable for a biosensing scenario (Fig. 5A/B). While longer polymers (predictably) improved saline stability to an extent that signals were very low/slow, (Fig. 5C/D). This serves to highlight the delicate balance between stability and sensing for metal nanoparticles where the glycan alone is not the only consideration but the macromolecular tether structure, which justifies the use of precision polymerisation methods.

A further library-oriented screen of 27 nanoparticle formulations (AuNP 30, 50, 70 nm; DP 10–50 in steps of 5 units) was used to identify the optimum size and linker length.[86] Initial saline stability screening determined that a linker length above DP25 was required to stabilise all particle sizes, therefore lower

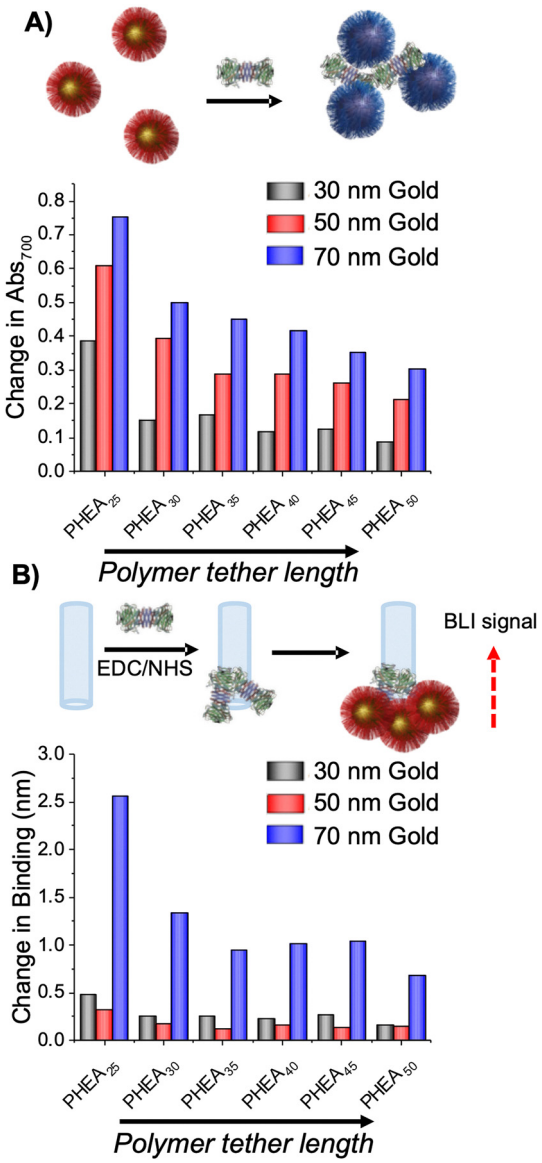

Fig. 6 Importance of polymer tether length and gold core size on the readout response by (A) aggregation of $GalNH_2$-functionalised AuNPs in response to 500 nM SBA and (B) biolayer interferometry using streptavidin coated biosensor with SBA immobilised in response to $GalNH_2$-functionalised AuNPs. Reproduced from ref. 86 with permission from American Chemical Society, copyright 2020.

DP polymers were omitted from follow on screening. To screen for binding, the GalNAc-binding lectin SBA (*soybean agglutinin)* was used to validate the methods and to establish which particle structural requirements gave the strongest outputs. For all polymer lengths, the largest changes were seen for the shortest polymer chain length (DP25) with a step-wise decrease as polymer length increases, and the biggest (70 nm) particles gave the largest outputs. It is important to note that individual glycans and lectins will give subtly different effects, but that the trends above are broadly true for lectin binding (Fig. 6A). The aggregation assay used above provides a convenient output of binding, but it cannot rule out the case where lectins bind but

fail to agglutinate: for example, the longer polymer linkers can bind to SBA, but also provide a steric block against agglutination, highlighting the need for tuning of these parameters. Therefore, a second assay using biolayer interferometry was developed to probe for false negatives. In short, biotinylated SBA was immobilised onto streptavidin functional BLI sensors and the nanoparticles exposed to this. The total BLI signal (which is essentially proportional to mass bound) as a function of particle parameters is shown in Fig. 6B. The shorter polymers at all particle sizes gave the largest output, highlighting how glycan accessibility is a crucial parameter but also that larger non-aggregating polymer coatings do bind, but without downstream signal generation.

Another important consideration is the optical density (standard method of reporting concentration) of the gold nanoparticle solution used. This is essential for reproducibility (as an easily accessible measurement), plus the probe concentration is expected to have a large impact on the signal outcomes.[87] At high concentrations of lectin, the signal begins to decrease due to saturation of the particle surface, so lectins only bind 1 particle (*i.e.* no cross-linking occurs) and hence no aggregation, therefore no signal. This is an important consideration to ensure lectins are tested in a concentration regime which allows true positive effects to be probed.

2.2. Impact of polymer structure

In addition to molecular weight, the architecture and chemical nature of multivalent systems will impact their outcomes.[88,89] Kiessling and coworkers showed the aggregation of mannose clusters (linear, dendritic) with Con A was architecture dependant, and the backbone-glycan linker can dramatically impact access into lectin binding sites.[90,91] Glycopolymer routing through dendritic cells is also shown to be antigen-size dependant.[92] We have explored how the exact chemical structure of the polymeric tether impacts outcomes, demonstrating that minor structural changes can dramatically impact biosensing success. For example, poly(*N*-(2-hydroxypropyl)methacrylamide) (PHPMA) is a widely used hydrophilic polymer and is accessible from RAFT polymerisation. We carried out a critical comparison of PHEA and PHPMA to ask if subtle differences in polymer structure would impact the signal detection outputs ?[93] Telechelic polymers were prepared by photoRAFT polymerisation to give a library of 30 particles with AuNP core sizes of 20, 30 and 40 nm and polymer lengths of ~DP25–75 ((Fig. 7A/B)). The first observation from this study was that that PHEA led to higher grafting densities than PHPMA (as revealed by comparative X-ray photoelectron spectroscopy (XPS)), attributable to the increased steric bulk associated with methyl on the backbone. Initial aggregation tests using Gal-PHPMA@AuNPs particles did not give any significant increase in Abs_{700}, but the PHEA equivalents did show aggregation (Fig. 7C/D). To a first approximation, this would be interpreted as 'no binding' for the PHPMA which is a surprise considering the presence of the galactose residue, but we considered this might be a false-negative due to the differences in polymer structure. It is perfectly feasible that binding can occur without cross-linking depending on the architecture of the glycans. To ensure that the above observations (no aggregation of Gal-PHPMA) was not due to inaccessibility of the glycan we used a complementary technique to assess lectin binding, BLI as described above. By comparing Gal-$PHPMA_{36}$@$AuNP_{40}$ (no aggregation response) with Gal-$PHEA_{33}$@$AuNP_{40}$ (strong aggregation response) we could clearly see that both particles have

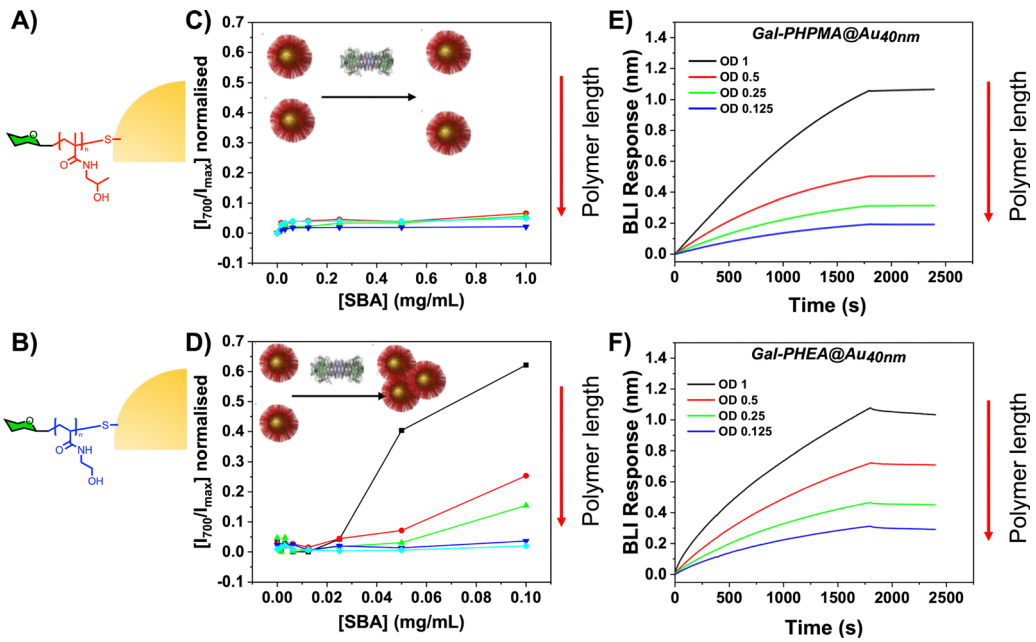

Fig. 7 Binding of nanoparticles with different polymeric tethers (A, B) with SBA. Measured by UV-visible spectroscopy: (A) Gal-$PHPMA_{36}$@$AuNP_{40}$ and (B) Gal-$PHEA_{33}$@$AuNP_{40}$. Biolayer interferometry analysis of nanoparticles binding to immobilised SBA in response to (E) Gal-$PHPMA_{36}$@$AuNP_{40}$ and (F) Gal-$PHEA_{33}$@$AuNP_{40}$. Reproduced from ref. 85 with permission from Royal Society of Chemistry, copyright 2020.

affinity towards the immobilised SBA with similar dose–response curves being obtained (Fig. 7E/F). This proves that the two polymer coatings both present sufficient Gal for strong SBA binding but that the PHPMA coating prevents aggregation from occurring, whereas PHEA encourages it. Taken together this study demonstrates that the chemical nature, as well as the molecular weight, of the polymer linker has a dramatic impact on the outcomes of glyconanoparticle sensing platforms, enabling control over aggregative *versus* non-aggregative outputs and will help design robust nano-biosensors in the future. It also highlights the need for complementary assays to determine binding profiles.

2.3. Glycan capture methods

A key consideration for the rationale design of modular glycan capturing ligands, is to use chemistry that is versatile, orthogonal and universal, and allows both small and larger branched glycans to be captured: in essence to take the inspiration of micro-array systems which allow automated glycan functionalisation and capture. Early examples of glycosylated nanoparticles from Cameron and co-workers synthesised glycosylated methacrylates which were polymerised by RAFT, before immobilisation on the gold (Fig. 8A). Such methods require multiple synthetic steps and column purification before polymerisation and when comparing two glycans it is challenging to obtain the same molecular weight and dispersity.[94] This led to post-polymerisation modification emerging as a powerful technology for systematic functionalisation of glycomaterials.[95] For example, Haddleton and co-workers used glycosyl azides to modify alkyne-functionalised pre-polymers using azide–alkyne click cycloadditions.[96] Other examples of the use of 'click'-type reactions include the following: thiol–ene,[97] thiol–yne,[98] thiol–chloro,[99] activated esters,[100,101] or thiolactones.[102] While convenient, the bottleneck is often the installation of the reactive handle onto the glycan. To overcome this challenge, Tanaka[103] and Fairbanks[104] have used imidazolinium salts to introduce azides at the reducing terminus directly from reducing glycans, allowing protecting-group free one-pot two-step glycosylations. Another appealing strategy for glycan conjugation is to exploit the hemiacetal equilibrium at the terminus of reducing glycans which can react with hydrazides. Glyconanoparticle/polymer libraries have been prepared using hydrazide functional polymers,[105–107] but there are significant challenges. The hydrazone bond is intrinsically dynamic so (depending on pH) the glycans can detach and exchange in a dynamic equilibrium.[108] Furthermore, the hydrazone linkage is an equilibrium between a ring-opened and ring-closed form. Chemical reduction (using, *e.g.*, $NaBH_4$) can increase stability but adds another step to the process. To overcome this, amino–oxy conjugates have emerged as alternatives due to their higher stability against hydrolysis[109,110] and at equilibrium exist in greater proportions as ring-closed structures (more like the native linkages) compared to hydrazides. We reported a method to generate glyconanoparticles from unprotected glycans by conjugation to polymer tethers bearing terminal amino–oxy groups, which are then immobilised onto gold nanoparticles. Using an ^{13}C enriched glycan, the efficiency of this reaction was probed in detail to confirm conjugation, with 25% of end-groups being functionalised, predominantly in the ring-closed form.[111] Whilst useful, this method's low conversion and more challenging synthesis make it less suitable for large scale use or in diagnostics (where residual hydrazide/aminooxy end groups may cross-react). Photochemical crosslinking methods based on perfluorophenyl azide have also been employed by Yan and co-workers.[112–114]

During our investigations, our modular polymer with a pentafluorophenyl (PFP) end-group was identified as being the most versatile and convenient handle, as it has been widely

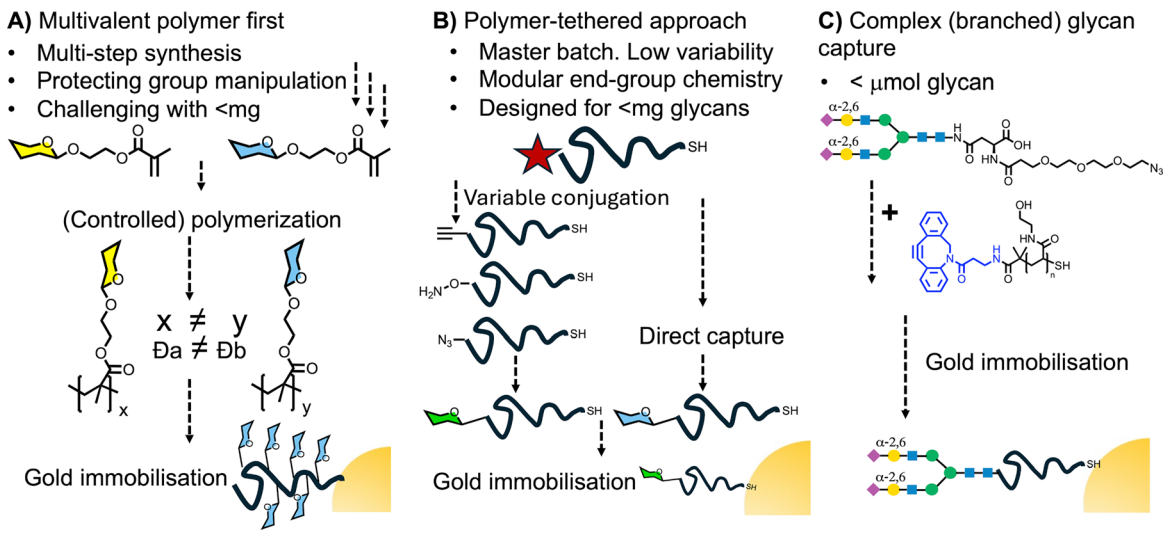

Fig. 8 Strategies for producing glycosylated AuNPs. (A) synthesis of polymers with pendant glycans, (B) glycan end-functionalised polymers, (C) incorporating more complex glycans on polymer end-terminus using bioorthogonal handles. All these approaches use a terminal thiol to immobilise into a gold particle.

used with amino-monosaccharides as a method for capturing glycans on the polymer terminus (Fig. 8B).[82,86,87,93,115–121] The PFP is appealing compared to other active esters (such as NHS) as it is more reactive and selective towards amines compared to alcohols or carboxylic acids, ensuring chemoselective ligation. The PFP group also has a unique signature in ^{19}F NMR, allowing reaction monitoring which is not always possible in ^{1}H NMR due to the large number of glycan peaks. This is particularly appealing with the rise of benchtop NMRs allowing for rapid and non-destructive reaction monitoring. Theato and co-workers pioneered the use of PFP in polymer science, incorporating these esters into acrylate and methacrylate monomers and polymerising using controlled radical methods such as RAFT polymerisation, producing well-defined polymers with reactive side groups. These polymers serve as versatile platforms for introducing diverse functionalities, efficiently and quantitatively under mild conditions (*e.g.*, room temperature).[122,123] This method has been used to produce glycopolymers for a range of lectin binding studies.[124,125]

A key consideration to note when using aminoglycans, is that they are typically obtained *via* the reduction of an azido-precursor. Therefore "click" chemistry strategies (to remove one glycan manipulation step) can accelerate nanoparticle preparation (Fig. 8C). The most versatile of these is copper-free strain-promoted alkyne-azide click (SPAAC), with dibenzocyclooctyne (DBCO) being the most used due to low cost and commercially availability.[126] By displacing the PFP with DBCO-NH_2 capture of rare glycans or sterically large is possible, which would be challenging with PFP, exemplified by the capture of mono- and bi-antennary azido sialyllactose and fluorinated Lewis^x glycans.[127–129] Budhadev *et al.* have used click methods to add multiple sugar ligands on a single short PEG tether, these clustered glycan arrangements accelerated nanoparticle aggregation in the presence of lectins compared to monovalent or sparsely distributed ligands, but can be more challenging to synthesise.[130]

The polymer-tethered glycosylated AuNPs are typically characterised using a range of complementary techniques, necessitated by the challenge of detecting very small amounts of surface ligands. UV-Vis spectroscopy, dynamic light scattering (DLS) and zeta potential measurements provide insights overall particle stability. Transmission electron microscopy (TEM) visualises core size and morphology but cannot typical probe the organic polymer coating. X-ray photoelectron spectroscopy (XPS) is a powerful tool which we have widely used for surface composition analysis of AuNPs providing chemical identity of the presence of the ligands. Thermogravimetric analysis (TGA) quantifies organic content without distinguishing glycan species but requires a large amount of material.[131] Nuclear magnetic resonance (NMR)[132] and mass spectrometry[133] can provide structural and compositional details.

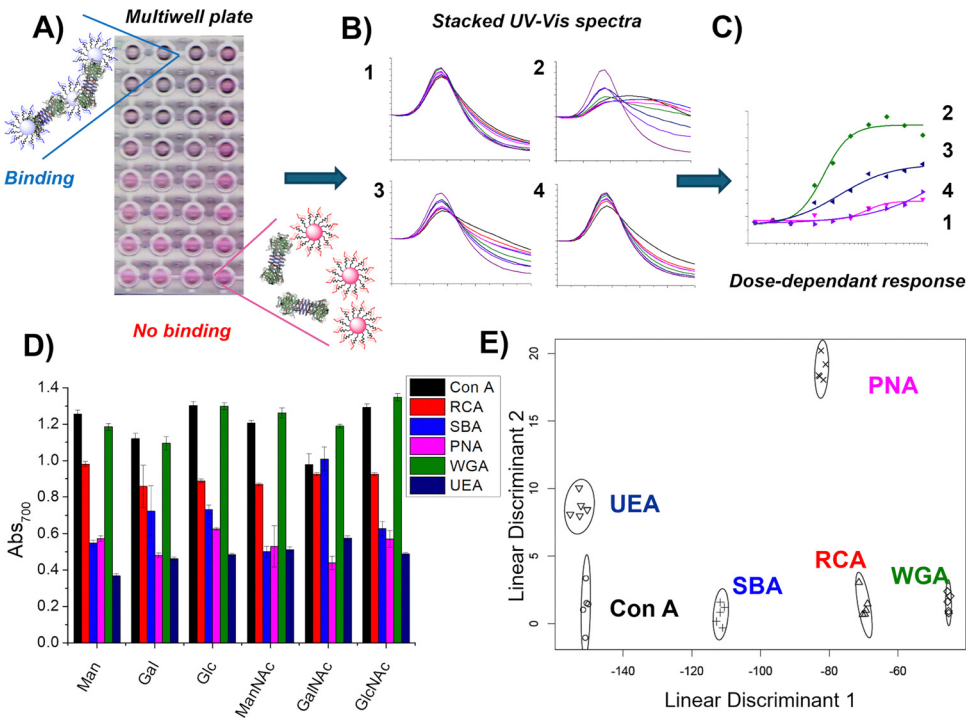

Fig. 9 High-throughput analysis using AuNPs and lectin discrimination. (A) Scanned image of a multiwell-plate with a serial dilution of a lectin in response to different glycosylated AuNPs, where purple/blue shows an interaction (aggregation) and pink/red is no interaction (no aggregation); (B) UV-vis traces of different glycosylated AuNPs in response to a serial dilution of a lectin; (C) binding isotherms from the absorbance measurement at 700 nm as a function of lectin concentration; (D) absorbance at 700 nm of Man-, Gal-, Glc-, ManNAc-, GalNAc- and GlcNAc-functionalised particles after 30 min incubation with 6.25 μg mL^{-1} Con A, RCA_{120}, SBA, WGA, PNA, UEA. Each is the average of five measurements; (E) linear discriminant plot showing excellent segregation between the six lectins. Reproduced from ref. 74 with permission from Royal Society of Chemistry, copyright 2014.

3. Glycosylated nanoparticles to dissect protein-glycan and protein unnatural-glycan interactions

The above sections summarise the synthetic development of polymer-tethered glycosylated gold nanoparticles, which was undertaken to unlock their biosensing capabilities. Understanding protein-carbohydrate interactions is crucial for drug design, vaccine development, and identifying disease biomarkers, as altered glycosylation patterns are linked to conditions like cancer and diabetes.[42,134] Additionally, insights into these interactions support advancements in biotechnology and industrial applications. Conventional approaches involve microarrays which require labelled proteins[135] or methods such as ITC which require relatively large amounts of sample and has limited throughput.[136] The polymer-tethered gold nanoparticle platform was identified as being a complementary technology, to explore the colorimetric responses of plasmonic gold cores with the modular nature of the polymer-steric stabilisers.[75,76,78,79,112,114,137] In an early demonstration Otten *et al.* prepared a library of seven monosaccharide-terminated polymers; mannose (Man), galactose (Gal), glucose (Glc), *N*-acetylmannosamine (ManNAc), *N*-acetylgalactosamine (GalNAc), *N*-acetylglucosamine (GlcNAc) and fucose (Fuc) using the hydrazide conjugation method.[106] This library was used to interrogate a panel of plant lectins: *concanavalin A* (Con A), *Ricinus communis* agglutinin (RCA_{120}, which is a non-toxic variant of ricin), *soybean agglutinin* (SBA), *peanut agglutinin* (PNA), *wheat germ agglutinin* (WGA) and *Ulex europaeus* agglutinin (UEA) in multiwell plates using aggregation (red-blue shift) as the output (Fig. 9A–D). Due to the volume of data generated with this tool, linear discriminant analysis (LDA) (Fig. 9E), a statistical and machine learning technique could be deployed to create 'barcodes' for multiplexed lectin detection, which has since been used with soluble polymers.[138]

An advantage of using polymeric tethers is that heterogeneous surfaces can be easily assembled through mixing, which to a first approximation mimics the complexity of the glycocalyx. Eleven combinations were prepared, from 100% galactosamine ($GalNH_2$) to 100% mannosamine ($ManNH_2$) in steps of 10%.[115] The post-polymerisation route employed means that all the polymers have the same initial chain length distribution and therefore reduced the variability between particle types, but allows versatile end-group functionalisation to make libraries of a variety of particles with differing carbohydrate densities. This heterogeneous display lead to improved discrimination between lectins which had otherwise similar binding preferences (SBA and RCA_{120}) for homogeneous glyconanoparticles (Fig. 10).[115]

The above examples were focussed on plant lectins and synthetically trivial monosaccharides, but the real potential of this approach is to explore more complex glycans and/or biomedically relevant glycan-binding partners. During the early stages of influenza infection, hemagglutinins on the viral surface engage sialic acids in their host. Simplistically, human influenza targets 2,6-linked sialic acids, but avian influenza targets 2,3-linked sialic acids, representing the abundance of each isomer in the host.[139,140] Zoonosis can occur when intermediate species, such as swine, presents both glycans allowing adaptation. We captured 2,6- and 2,3-sialyllactose onto PHEA tethers and assembled them onto the gold nanoparticles and used these to interrogate hemagglutinins from a range of influenza strains.[86] Using hemagglutinins bound to BLI (biolayer interferometry) sensors it was possible to rapidly assess binding preference, which was in line with the microarray data, showing the potential for these particles for rapid evaluation of viral threats. In 2020 when SARS-CoV-2 emerged, it was unknown if, or which, glycans it would bind to during initial stage of infection and represented a significant knowledge gap. Guided by the above influenza work, Baker *et al.* used polymer-tethered nanoparticles to discover that SARS-CoV-2 binds sialic acids (Fig. 11), which was validated by complimentary modelling and STD NMR[117] and also by using anisotropic gold nanoparticle probes.[121] These

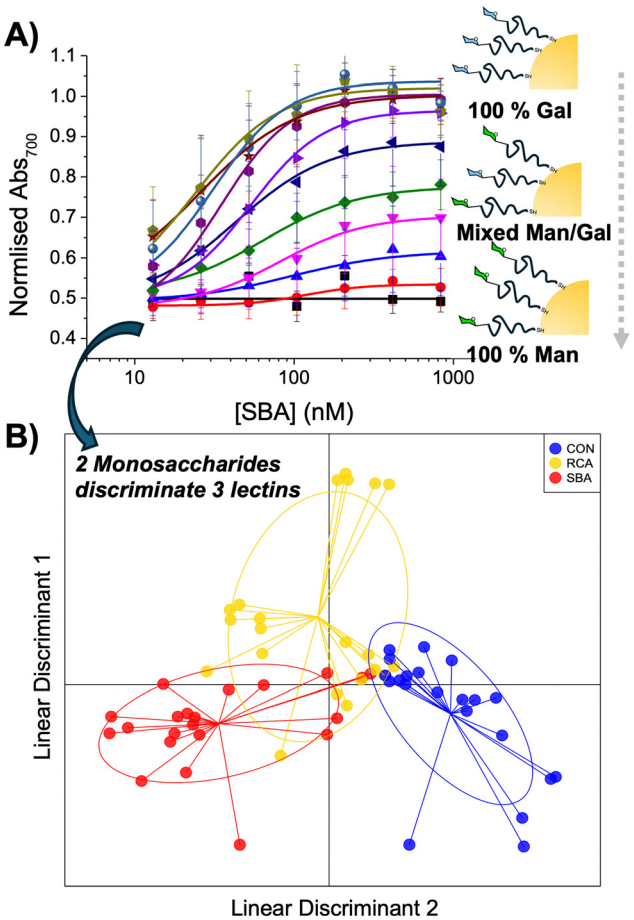

Fig. 10 (A) Dose-dependent binding isotherms of mixed Man/Gal@AuNPs in response to a serial dilution of SBA. (B) The LDA model generated to discriminate between Con A, RCA_{120} and SBA from mixed Man/Gal@AuNPs. In the model each point represents a sample of that lectin and the ellipse represents one standard deviation from the average. Reproduced from ref. 115 with permission from Royal Society of Chemistry, copyright 2016.

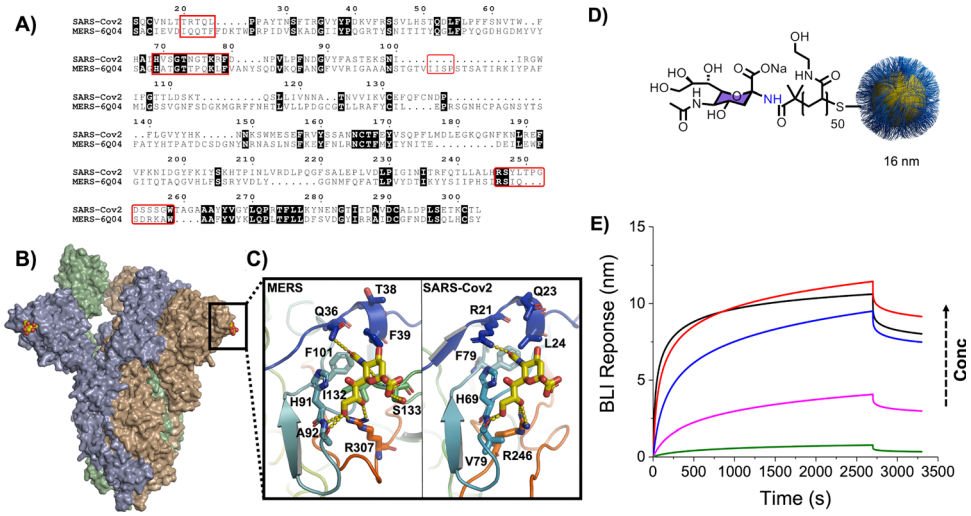

Fig. 11 (A) Sequence alignment between the S1 domains of the SARS-CoV-2 and MERS spike proteins. Regions important for sialic acid binding are highlighted by red boxes; (B) model showing the hypothesised sialic acid binding sites (yellow CPK colouring) for the SARS-CoV-2 spike protein trimer; (C) a comparison between the sialic acid binding sites from MERS (PDB entry 6Q04) and the SARS-COV-2 model (PDB entry 6VSB) in complex with a 2,3′-sialyllactose. Biolayer interferometry analysis of SARS-COV-2 spike protein with glyconanoparticles. (D) NeuNAc functionalised 16 nm AuNPs (NeuNAc-PHEA$_{50}$@AuNP$_{16}$) (E) biolayer interferometry analysis of SARS-CoV-2 spike protein with serial dilution of NeuNAc-PHEA$_{50}$@AuNP$_{16}$. Reproduced from ref. 117 with permission from American Chemical Society, copyright 2020.

observations were later confirmed by others[141,142] and used to develop multivalent sialic acid decoys as potential anti-adhesion agents.[143]

The above examples of generating signal outputs upon glycan/protein binding showed potential of this platform but had been limited to glycans of low complexity and mostly with known and well-characterised binding partners which were all available at unchallenging (mg) scale. An advantage of the modular nanoparticle platform compared to *e.g.* microarrays, is that it is also suitable for smaller numbers of glycans

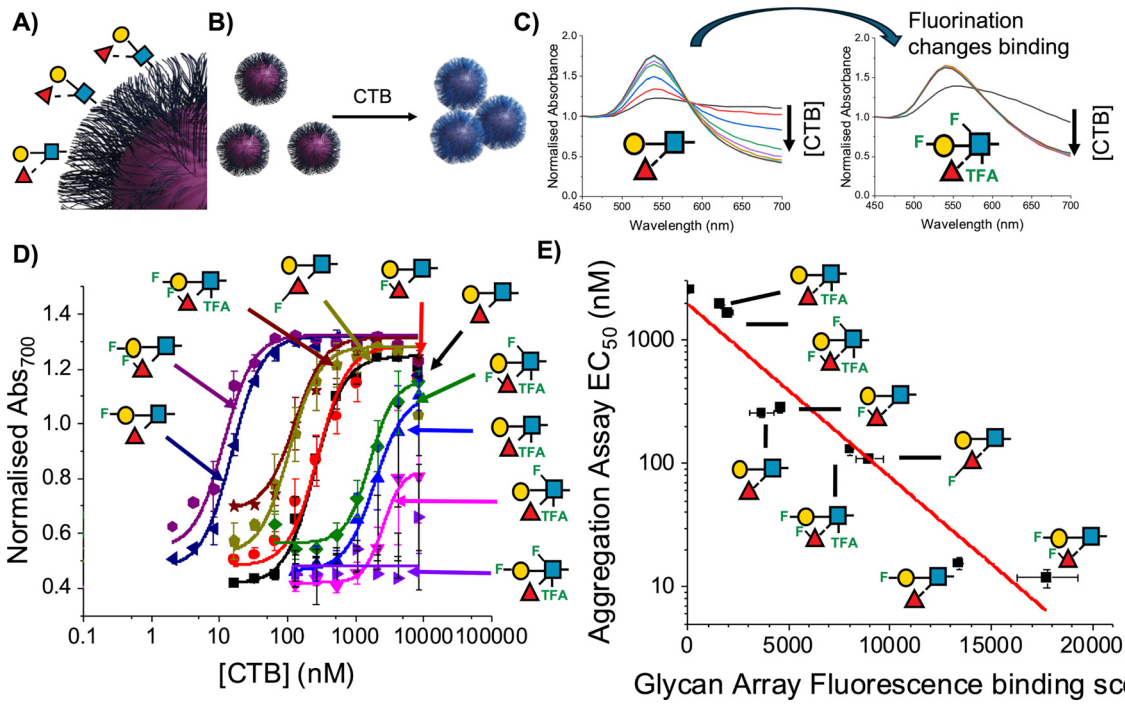

Fig. 12 (A) Lewis^x-functionalised AuNPs nanoparticles; (B) principle of detection due to gold nanoparticle red-blue shift upon aggregation with CTB; (C) UV-visible spectra for gold nanoparticles with native Lewis^x (**LeX1**) and fluorinated **LeX22**; (D) dose-dependent response of library of Lewis^x glyconanoparticles to CTB. Data is presented as mean normalised Abs$_{700}$ from UV-visible spectroscopy ± standard error of 3 replicates. (E) Correlation of glycan array and glyconanoparticle binding data. Reproduced from ref. 129 with permission from Springer Nature, copyright 2024.

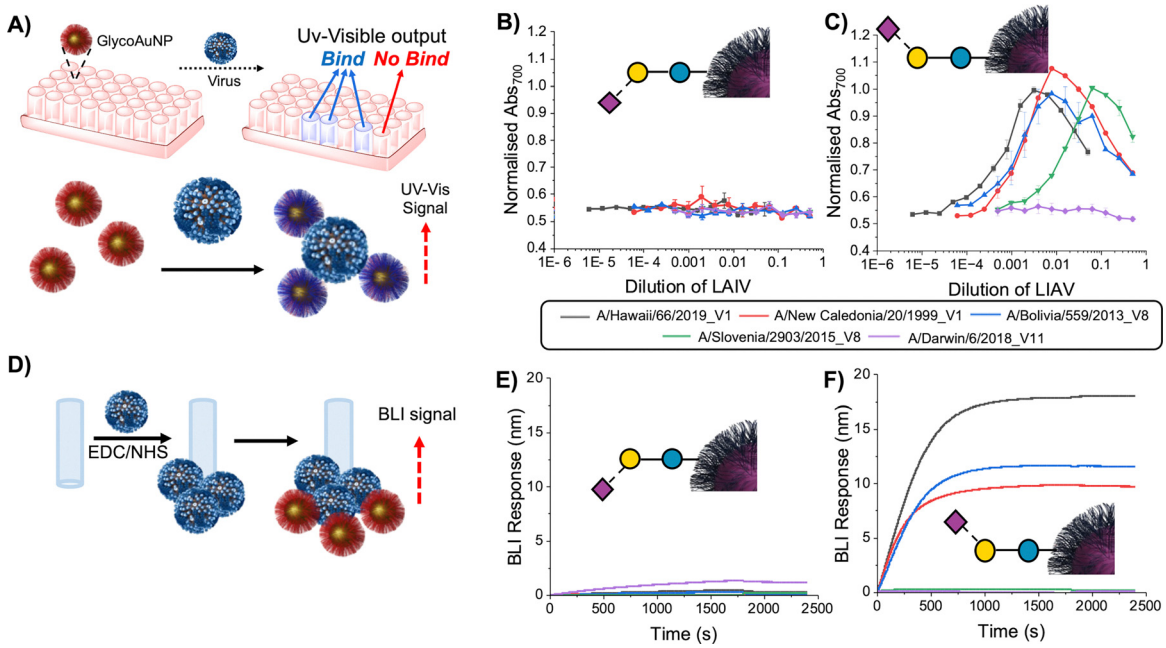

Fig. 13 Sialyllactose-functional nanoparticles binding to the live attenuated influenza vaccine (LAIV) virus. (A) Schematic representation of the aggregation assay, where GlycoAuNP particles cross-linking virus; (B) dose-response of LAIV viruses *versus* 2,3 sialyllactose AuNPs; (C) dose-response of LAIV viruses *versus* 2,6 sialyllactose AuNPs; Error bars are the standard error of the mean from n = 3. (D) Schematic representation of the BLI assay with immobilisation of the LAIV virus to the sensor; (E) BLI response of LAIV virus to 2,3 SL AuNPs; (F) BLI response of LAIV virus *versus* 2,6 SL AuNPs. BLI was undertaken at 0.375× dilution of LAIV virus with AuNPs at OD_{540} (optical density@540 nm) = 1. In all assays, neuraminidase inhibitors, 25 μM oseltamivir carboxylate and 100 μM zanamivir, were used. Reproduced from ref. 127 with permission from Wiley-VCH GmbH, copyright 2025.

(*e.g.* 1–10), whereas microarrays' power scales with the number of targets. Using chemoenzymatic synthesis nine sequentially modified fluoro-lacto-*N*-biose glycans were prepared and captured onto the particles, achieved using μg quantitates, with conjugation demonstrated using X-ray photoelectron spectroscopy (XPS) due to the limited amounts where *e.g.* NMR would not be appropriate. Using the colourimetric aggregation assay it was shown how the precise location of the fluorine atom impacted binding towards two galectins (galectin-3 and galectin-7, galectin-1 showed no binding to any of the probes), and led to increased selectivity, with a tetra-fluorinated lacto-*N*-biose showing a complete switch in affinity between galectin-3 and -7.[128] This work was further expanded for the study of fluorinated Lewis^x glycans, including a side-by-side comparison of the nanoparticle approach with convention lipid-linked microarrays studies, for the first time (Fig. 12).[129] This side-by-side analysis showed close correlation between IC_{50} (nanoparticles) and total signal (arrays) in binding to the cholera toxin, showing how fluorination could drive a 1000-fold difference in IC_{50}. These particles were also shown, in a proof-of-concept, to be suitable for lateral flow glyco detection of the cholera toxin.

The above examples were limited to trisaccharides as the largest glycan cargo, but to be truly competitive and complimentary to array-based technologies large and branched glycans are also required. Chemoenzymatic synthesis was used to make unnatural biantennary glycans (2 trisaccharide arms) and these were successfully captured and immobilised using both amine-PFP and 'click' coupling routes.[127] The particles were optimised to generate signal in the presence of whole virus (in this case, vaccine-strain influenzas) meaning glycan-binding preferences could be extracted by simple colourimetric changes in a microplate (Fig. 13). Compared to arrays, this technology can be deployed *in situ* in a biosafety hood (for example) without needing to move to a central array platform and can be considered a new bench-side tool. The sterically large glycans did not impact the overall stability of the particles, showing the polymer tethers performed this steric stabilisation role even with large end-groups. These interactions were studied in the presence of neuraminidase inhibitors (oseltamivir carboxylate and zanamivir), ensuring results were not biased by neuraminidase cleavage of sialic acids. Due to glycosidic *O*-linkages being prone to cleavage by glycosidases in biological fluids, risking premature loss of glycan ligands before they engage their targets, alternative, enzyme-resistant linkages such as *C*-glycosides which retain their conformation have been explored.[144,145]

4. Lateral flow diagnostics

A lateral flow device (LFD) is a rapid diagnostic tool commonly used for point-of-care testing. It is a self-contained paper-based device designed to detect the presence (or absence) of a target analyte in a liquid sample. LFDs are often used for medical diagnostics, food safety, and environmental testing. LFDs

typically rely on antibodies as recognition units, owing to their high specificity. A typical LFD has antibody immobilised on both the mobile phase (gold particle) and stationary phase (nitrocellulose) forming a 'sandwich' around the antigen, to generate the characteristic red line, due to concentration of the gold nanoparticles. Glycans offer an alternative to these recognition units, and their study might bring new opportunities.[146] There are synthetic and ethical advantages to using glycans over antibodies: glycans can be cheaper to produce in large quantities synthetically or chemoenzymatically *via* animal-free routes and they are thermally stable. However, despite this, there are only few examples of glyco-LFDs. Damborský *et al.* demonstrated a lectin-based LFD to detect aberrantly glycosylated prostate-specific antigen.[147] Miura and co-workers developed a flow-through method for detecting Shiga Toxin-1, which was deposited on the nitrocellulose and binding was observed with galactosylated AuNPs.[124] This was taken further by using mannosylated-AuNPs to detect Con A.[79] In this case, the glyconanoparticles were used in the mobile phase and a rabbit anti-Con A antibody as the stationary phase test line with a further study varying to mannose density to optimisation of the readout.[78] Whilst not a full glycoLFD, this study clearly demonstrated that glycoLFDs are possible. Hernando *et al.* used glycan–BSA conjugates on gold nanoparticles to detect the ricin surrogate RCA_{120}.[148] Kim *et al.* exploited SARS-CoV-2's ability to bind glycosaminoglycans to develop *GlycoGrip* a glycopolymer capture line for SARS-CoV-2 which was used with anti-spike antibody coated AuNPs as the mobile phase.[149]

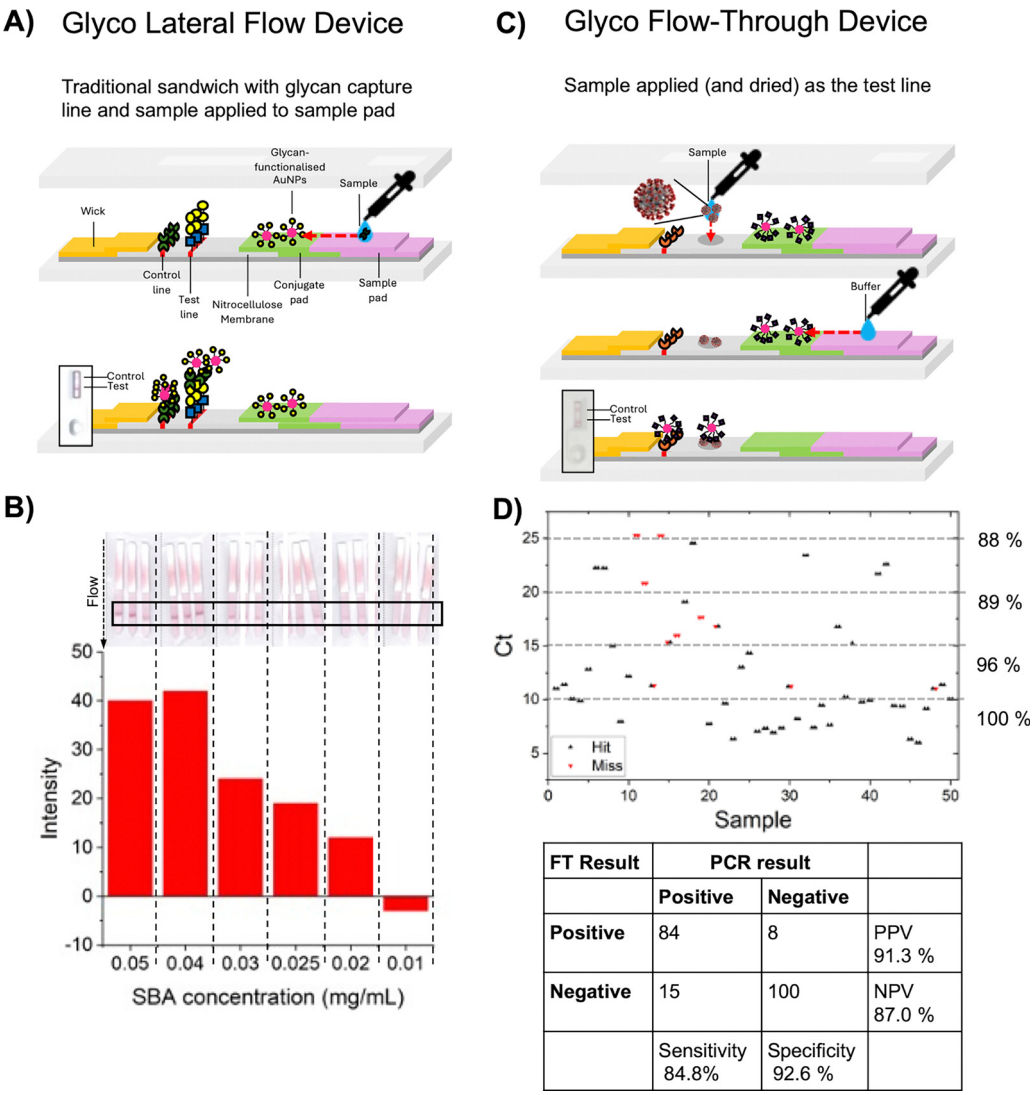

FT Result	PCR result		
	Positive	**Negative**	
Positive	84	8	PPV 91.3 %
Negative	15	100	NPV 87.0 %
	Sensitivity 84.8%	Specificity 92.6 %	

Fig. 14 (A) Representative lateral flow glyco-assay and for SBA. Reproduced from ref. 146 with permission from American Chemical Society, copyright 2022. (B) Lateral flow dipsticks run with the indicated concentrations of SBA using Gal-$PHEA_{72}$@$AuNP_{16}$. Reproduced from ref. 119 with permission from Wiley-VCH GmbH, copyright 2022. (C) Representative flow-through glyco-assay for sensing SARS-CoV-2. Reproduced from ref. 146 with permission from American Chemical Society, copyright 2022 (D) results of flow-through device performance (hit or miss) as a function of Ct (PCR threshold cycles) for heat-inactivated primary patient swabs devices. Thresholds indicated are the sensitivity as a function of the Ct value. Confusion matrices. Sensitivity = TP/(TP + FN); specificity = TN/(TN + FP); PPV = TP/(TP + FP); NPV = TN/(TN + FN). TP = true positive; TN = true negative; FN = false negative; and FP = false positive. Reproduced from ref. 118 with permission from American Chemical Society, copyright 2021.

Our team set out to make complete lateral flow *glyco* diagnostics[146] where the stationary and mobile phases comprised of glycans (Fig. 14A). In excess of 30 polymer-tethered glycosylated nanoparticles were optimised for chain length and nanoparticle core to avoid unwanted aggregation (which could lead to both false negatives and false positives) using galactosylated probes and glycosylated-BSA as the stationary phase.[119] This set up allowed lectin detection at nM concentrations which was comparable to commercial antibody-LFDs (Fig. 14B).[119] Further optimisation using glycosylated poly(vinyl pyrrolidone)amphiphilic anchors for the stationary phase enable construction of an ''all glycopolymer'' lateral flow device for lectin detection, showing how all biologic materials can be replaced with precision synthetic polymers.[150] A key advantage of antibody-LFDs is that they have been extensively optimised for use with complex media, such as saliva, which is far more challenging than proof of principal in buffer. To allow primary clinical swabs to be used, we used a flow-through assay (Fig. 14C), where by the clinical sample is dried as the stationary phase, and the mobile glyco-particles ''flowed over'': in this set up SARS-CoV-2 diagnostics were shown with a panel of 100 clinical swabs, resulted in sensitivity of 85% and specificity of 93%,[118] fully demonstrating that glyco-diagnostics can be rapidly assembled for pathogen detection (Fig. 14D).

4. Conclusions

Here we have summarised the development process of polymer-tethered glyconanoparticles within our laboratory and their emerging role in glycobiology. The synthetic requirements for a useful polymer tether were covered in detail, including the chemistry and molecular weight requirements and the potential benefits of using RAFT-polymerisation chemistry to exploit the inevitable *thio* end groups for gold particle immobilisation. Glycan capture technologies, which now enable μg quantities of precious glycans to be conjugated to polymers were highlighted, with specific examples of fluorinated glycans used. The use of these in biosensing, from colourimetric aggregation assays to surface-coupled detection is discussed and comparisons drawn to established (printed) array technologies. The potential of these as the mobile phase of a new class of lateral flow *glyco* diagnostics is shown with specific examples including SARS-COV-2 detection. The challenges of translation are also shown, with particular focus on particle stability in complex media and non-specific binding. This technology is now at a stage where it is simple to use and can probe unknown binding events and is inherently compatible with automation strategies, in cases where sufficient glycan diversity is available.

As an outlook of this technology, the following challenges/opportunities remain to be addressed in the opinion of the authors:

(i) Full automation of the glycan addition, coating and running of assays to unlock high throughput screening, comparable to solid-phase microarrays.

(ii) Deployment of anisotropic particles to allow non-crosslinking targets to be detected and improved detection limits.

(iii) Reducing the non-specific binding which can bring unwanted 'glyco-coronas' to the particles.[151]

(iv) Overcoming the selectivity challenges in using glycans in *real world* diagnostics, which may include hybrid devices incorporating both antibodies and glycans.

(v) Using the synthetic versatility to introduce dynamic glycan presentation in response to stimuli for controlled and triggerable 'revealing' of specific glycans with spatio-temporal control.[152]

Conflicts of interest

There are no conflicts of interest to declare.

Data availability

This is a review-type article and contains no new data.

Acknowledgements

The authors thank the University of Manchester for funding. We also thank our previous and ongoing collaborators in this field and current/former group members for their contributions.

References

1 A. Varki, Biological Roles of Glycans, *Glycobiology*, 2017, **27**(1), 3–49, DOI: 10.1093/glycob/cww086.
2 K. T. Pilobello and L. K. Mahal, Deciphering the Glycocode: The Complexity and Analytical Challenge of Glycomics, *Curr. Opin. Chem. Biol.*, 2007, **11**(3), 300–305, DOI: 10.1016/j.cbpa.2007.05.002.
3 J. J. Lundquist and E. J. Toone, The Cluster Glycoside Effect, *Chem. Rev.*, 2002, **102**(2), 555–578, DOI: 10.1021/cr000418f.
4 Y. C. Lee, R. R. Townsend, M. R. Hardy, J. Lönngren, J. Arnarp, M. Haraldsson and H. Lönn, Binding of Synthetic Oligosaccharides to the Hepatic Gal/GalNAc Lectin. Dependence on Fine Structural Features, *J. Biol. Chem.*, 1983, **258**(1), 199–202, DOI: 10.1016/S0021-9258(18)33240-X.
5 Y. C. Lee and R. T. Lee, Carbohydrate-Protein Interactions: Basis of Glycobiology, *Acc. Chem. Res.*, 1995, **28**(8), 321–327, DOI: 10.1021/ar00056a001.
6 C. R. Bertozzi and L. L. Kiessling, Chemical Glycobiology, *Science*, 2001, **291**(5512), 2357–2364, DOI: 10.1126/science.1059820.
7 M. Mammen, S.-K. Choi and G. M. Whitesides, Polyvalent Interactions in Biological Systems: Implications for Design and Use of Multivalent Ligands and Inhibitors, *Angew. Chem., Int. Ed.*, 1998, **37**(20), 2754–2794, DOI: 10.1002/(SICI)1521-3773(19981102)37:20%253C2754::AID-ANIE2754%253E3.0.CO;2-3.
8 Á. G. Barrientos, J. M. de la Fuente, T. C. Rojas, A. Fernández and S. Penadés, Gold Glyconanoparticles: Synthetic Polyvalent Ligands Mimicking Glycocalyx-Like Surfaces as Tools for Glycobiological Studies, *Chem. – Eur. J.*, 2003, **9**(9), 1909–1921, DOI: 10.1002/chem.200204544.
9 S. Dedola, M. D. Rugen, R. J. Young and R. A. Field, Revisiting the Language of Glycoscience: Readers, Writers and Erasers in Carbohydrate Biochemistry, *ChemBioChem*, 2020, **21**(3), 423–427, DOI: 10.1002/cbic.201900377.
10 J. M. Rini, K. W. Moremen, B. G. Davis and J. D. Esko, in Glycosyltransferases and Glycan-Processing Enzymes, *Essentials of Glycobiology*, ed A. Varki, R. D. Cummings, J. D. Esko, P. Stanley, G. W. Hart, M. Aebi, D. Mohnen, T. Kinoshita, N. H. Packer,

J. H. Prestegard, R. L. Schnaar and P. H. Seeberger, Cold Spring Harbor Laboratory Press, Cold Spring Harbor (NY), 2022.
11 E. Sterner, N. Flanagan and J. C. Gildersleeve, Perspectives on Anti-Glycan Antibodies Gleaned from Development of a Community Resource Database, *ACS Chem. Biol.*, 2016, **11**(7), 1773–1783, DOI: 10.1021/acschembio.6b00244.
12 K. M. Gillmann, J. S. Temme, S. Marglous, C. E. Brown and J. C. Gildersleeve, Anti-Glycan Monoclonal Antibodies: Basic Research and Clinical Applications, *Curr. Opin. Chem. Biol.*, 2023, **74**, 102281, DOI: 10.1016/j.cbpa.2023.102281.
13 A. Adibekian, P. Stallforth, M.-L. Hecht, D. B. Werz, P. Gagneux and P. H. Seeberger, Comparative Bioinformatics Analysis of the Mammalian and Bacterial Glycomes, *Chem. Sci.*, 2011, **2**(2), 337–344, DOI: 10.1039/C0SC00322K.
14 M. C. Galan, D. Benito-Alifonso and G. M. Watt, Carbohydrate Chemistry in Drug Discovery, *Org. Biomol. Chem.*, 2011, **9**(10), 3598–3610, DOI: 10.1039/C0OB01017K.
15 R. A. Dwek, Glycobiology: Toward Understanding the Function of Sugars, *Chem. Rev.*, 1996, **96**(2), 683–720, DOI: 10.1021/cr940283b.
16 J. Hirabayashi, Lectin-Based Structural Glycomics: Glycoproteomics and Glycan Profiling, *Glycoconj J.*, 2004, **21**(1), 35–40, DOI: 10.1023/B:GLYC.0000043745.18988.a1.
17 J. A. Prescher and C. R. Bertozzi, Chemical Technologies for Probing Glycans, *Cell*, 2006, **126**(5), 851–854, DOI: 10.1016/j.cell.2006.08.017.
18 J. E. Turnbull and R. A. Field, Emerging Glycomics Technologies, *Nat. Chem. Biol.*, 2007, **3**(2), 74–77, DOI: 10.1038/nchembio0207-74.
19 R. D. Cummings and J. D. Esko, in Principles of Glycan Recognition, *Essentials of Glycobiology*, ed A. Varki, R. D. Cummings, J. D. Esko, H. H. Freeze, P. Stanley, C. R. Bertozzi, G. W. Hart and M. E. Etzler, Cold Spring Harbor Laboratory Press, Cold Spring Harbor (NY), 2009.
20 J. Hirabayashi, M. Yamada, A. Kuno and H. Tateno, Lectin Microarrays: Concept, Principle and Applications, *Chem. Soc. Rev.*, 2013, **42**(10), 4443–4458, DOI: 10.1039/C3CS35419A.
21 J. P. Ribeiro and L. K. Mahal, Dot by Dot: Analyzing the Glycome Using Lectin Microarrays, *Curr. Opin. Chem. Biol.*, 2013, **17**(5), 827–831, DOI: 10.1016/j.cbpa.2013.06.009.
22 J. Angulo, A. Ardá, S. Bertuzzi, A. Canales, J. Ereño-Orbea, A. Gimeno, M. Gomez-Redondo, J. C. Muñoz-García, P. Oquist, S. Monaco, A. Poveda, L. Unione and J. Jiménez-Barbero, NMR Investigations of Glycan Conformation, Dynamics, and Interactions, *Prog. Nucl. Magn. Reson. Spectrosc.*, 2024, **144–145**, 97–152, DOI: 10.1016/j.pnmrs.2024.10.002.
23 C. J. Gray, B. Schindler, L. G. Migas, M. Pičmanová, A. R. Allouche, A. P. Green, S. Mandal, M. S. Motawia, R. Sánchez-Pérez, N. Bjarnholt, B. L. Møller, A. M. Rijs, P. E. Barran, I. Compagnon, C. E. Eyers and S. L. Flitsch, Bottom-Up Elucidation of Glycosidic Bond Stereochemistry, *Anal. Chem.*, 2017, **89**(8), 4540–4549, DOI: 10.1021/acs.analchem.6b04998.
24 C. J. Gray, L. G. Migas, P. E. Barran, K. Pagel, P. H. Seeberger, C. E. Eyers, G.-J. Boons, N. L. B. Pohl, I. Compagnon, G. Widmalm and S. L. Flitsch, Advancing Solutions to the Carbohydrate Sequencing Challenge, *J. Am. Chem. Soc.*, 2019, **141**(37), 14463–14479, DOI: 10.1021/jacs.9b06406.
25 C. J. Gray, I. Compagnon and S. L. Flitsch, Mass Spectrometry Hybridized with Gas-Phase InfraRed Spectroscopy for Glycan Sequencing, *Curr. Opin. Struct. Biol.*, 2020, **62**, 121–131, DOI: 10.1016/j.sbi.2019.12.014.
26 M. S. M. Timmer, B. L. Stocker and P. H. Seeberger, Probing Glycomics, *Curr. Opin. Chem. Biol.*, 2007, **11**(1), 59–65, DOI: 10.1016/j.cbpa.2006.11.040.
27 T. Feizi, M. S. Stoll, C. T. Yuen, W. Chai and A. M. Lawson, Neoglycolipids: Probes of Oligosaccharide Structure, Antigenicity, and Function, *Methods Enzymol.*, 1994, **230**, 484–519, DOI: 10.1016/0076-6879(94)30030-5.
28 R. A. Childs, A. S. Palma, S. Wharton, T. Matrosovich, Y. Liu, W. Chai, M. A. Campanero-Rhodes, Y. Zhang, M. Eickmann, M. Kiso, A. Hay, M. Matrosovich and T. Feizi, Receptor-Binding Specificity of Pandemic Influenza A (H1N1) 2009 Virus Determined by Carbohydrate Microarray, *Nat. Biotechnol.*, 2009, **27**(9), 797–799, DOI: 10.1038/nbt0909-797.
29 M. Sojitra, S. Sarkar, J. Maghera, E. Rodrigues, E. J. Carpenter, S. Seth, D. Ferrer Vinals, N. J. Bennett, R. Reddy, A. Khalil, X. Xue, M. R. Bell, R. B. Zheng, P. Zhang, C. Nycholat, J. J. Bailey, C.-C. Ling, T. L. Lowary, J. C. Paulson, M. S. Macauley and R. Derda, Genetically Encoded Multivalent Liquid Glycan Array Displayed on M13 Bacteriophage, *Nat. Chem. Biol.*, 2021, **17**(7), 806–816, DOI: 10.1038/s41589-021-00788-5.
30 C. R. Bertozzi, Bioorthogonal Chemistry: Fishing for Selectivity in a Sea of Functionality, *Angew. Chem., Int. Ed.*, 2010, **48**(38), 6974–6998, DOI: 10.1002/anie.200900942.Bioorthogonal.
31 M. Kufleitner, L. M. Haiber and V. Wittmann, Metabolic Glycoengineering – Exploring Glycosylation with Bioorthogonal Chemistry, *Chem. Soc. Rev.*, 2023, **52**(2), 510–535, DOI: 10.1039/D2CS00764A.
32 R. M. F. Tomás and M. I. Gibson, 100th Anniversary of Macromolecular Science Viewpoint: Re-Engineering Cellular Interfaces with Synthetic Macromolecules Using Metabolic Glycan Labeling, *ACS Macro Lett.*, 2020, **9**(7), 991–1003, DOI: 10.1021/acsmacrolett.0c00317.
33 Y. Y. Lam, A. Tan, C. J. Nowell, K. Kempe and B. J. Boyd, Systematic Investigation of Metabolic Oligosaccharide Engineering Efficiency in Intestinal Cells Using a Dibenzocyclooctyne-Monosaccharide Conjugate, *ChemBioChem*, 2023, **24**(12), e202300144, DOI: 10.1002/cbic.202300144.
34 M. M. B. Helmeke, R. L. Haynie-Cion and M. R. Pratt, Achieving Cell-Type Selectivity in Metabolic Oligosaccharide Engineering, *RSC Chem. Biol.*, 2025, **6**(10), 1506–1520, DOI: 10.1039/D5CB00168D.
35 A. Cioce, G. Bineva-Todd, A. J. Agbay, J. Choi, T. M. Wood, M. F. Debets, W. M. Browne, H. L. Douglas, C. Roustan, O. Y. Tastan, S. Kjaer, J. T. Bush, C. R. Bertozzi and B. Schumann, Optimization of Metabolic Oligosaccharide Engineering with Ac_4 GalNAlk and Ac_4 GlcNAlk by an Engineered Pyrophosphorylase, *ACS Chem. Biol.*, 2021, **16**(10), 1961–1967, DOI: 10.1021/acschembio.1c00034.
36 R. A. Flynn, K. Pedram, S. A. Malaker, P. J. Batista, B. A. H. Smith, A. G. Johnson, B. M. George, K. Majzoub, P. W. Villalta, J. E. Carette and C. R. Bertozzi, Small RNAs Are Modified with N-Glycans and Displayed on the Surface of Living Cells, *Cell*, 2021, **184**(12), 3109–3124.e22, DOI: 10.1016/j.cell.2021.04.023.
37 Y.-S. Liu, Y.-L. Miao, Y. Dou, Z.-H. Yang, W. Sun, X. Zhou, Z. Li, N. Hideki, X.-D. Gao and M. Fujita, Processing of N-Glycans in the ER and Golgi Influences the Production of Surface Sialylated glycoRNA, *Glycoconj J.*, 2024, **41**(6), 361–370, DOI: 10.1007/s10719-024-10171-w.
38 J. Porat, C. P. Watkins, C. Jin, X. Xie, X. Tan, C. G. Lebedenko, H. Hemberger, W. Shin, P. Chai, J. J. Collins, B. A. Garcia, D. Bojar and R. A. Flynn, O-Glycosylation Contributes to Mammalian glycoRNA Biogenesis, *bioRxiv*, preprint, 2024.08.28.610074, 2024, DOI: 10.1101/2024.08.28.610074.
39 D. H. Dube and C. R. Bertozzi, Metabolic Oligosaccharide Engineering as a Tool for Glycobiology, *Curr. Opin. Chem. Biol.*, 2003, **7**(5), 616–625, DOI: 10.1016/j.cbpa.2003.08.006.
40 J. Heimburg-Molinaro, A. Y. Mehta, C. A. Tilton and R. D. Cummings, Insights Into Glycobiology and the Protein-Glycan Interactome Using Glycan Microarray Technologies, *Mol. Cell. Proteomics*, 2024, **23**(11), 100844, DOI: 10.1016/j.mcpro.2024.100844.
41 E. Rodríguez, S. T. T. Schetters and Y. Van Kooyk, The Tumour Glyco-Code as a Novel Immune Checkpoint for Immunotherapy, *Nat. Rev. Immunol.*, 2018, **18**(3), 204–211, DOI: 10.1038/nri.2018.3.
42 A. Magalhães, H. O. Duarte and C. A. Reis, Aberrant Glycosylation in Cancer: A Novel Molecular Mechanism Controlling Metastasis, *Cancer Cell*, 2017, **31**(6), 733–735, DOI: 10.1016/j.ccell.2017.05.012.
43 J. Poole, C. J. Day, M. von Itzstein, J. C. Paton and M. P. Jennings, Glycointeractions in Bacterial Pathogenesis, *Nat. Rev. Microbiol.*, 2018, **16**(7), 440–452, DOI: 10.1038/s41579-018-0007-2.
44 S. S. Pinho, I. Alves, J. Gaifem and G. A. Rabinovich, Immune Regulatory Networks Coordinated by Glycans and Glycan-Binding Proteins in Autoimmunity and Infection, *Cell Mol. Immunol.*, 2023, **20**(10), 1101–1113, DOI: 10.1038/s41423-023-01074-1.
45 F. I. Mohideen and L. K. Mahal, Infection and the Glycome–New Insights into Host Response, *ACS Infect. Dis.*, 2024, **10**(8), 2540–2550, DOI: 10.1021/acsinfecdis.4c00315.
46 K. L. Kelly, E. Coronado, L. L. Zhao and G. C. Schatz, The Optical Properties of Metal Nanoparticles: The Influence of Size, Shape, and Dielectric Environment, *J. Phys. Chem. B*, 2003, **107**(3), 668–677, DOI: 10.1021/jp026731y.
47 L. Dykman and N. Khlebtsov, Gold Nanoparticles in Biomedical Applications: Recent Advances and Perspectives, *Chem. Soc. Rev.*, 2012, **41**(6), 2256–2282, DOI: 10.1039/c1cs15166e.

48 J. E. Ghadiali and M. M. Enzyme-Responsive Nanoparticle Systems Stevens, *Adv. Mater.*, 2008, **20**(22), 4359–4363, DOI: 10.1002/adma.200703158.
49 A. Svärd, J. Neilands, E. Palm, G. Svensäter, T. Bengtsson and D. Aili, Protein-Functionalized Gold Nanoparticles as Refractometric Nanoplasmonic Sensors for the Detection of Proteolytic Activity of Porphyromonas Gingivalis, *ACS Appl. Nano Mater.*, 2020, **3**(10), 9822–9830, DOI: 10.1021/acsanm.0c01899.
50 A. Laromaine, L. Koh, M. Murugesan, R. V. Ulijn and M. M. Stevens, Protease-Triggered Dispersion of Nanoparticle Assemblies, *J. Am. Chem. Soc.*, 2007, **129**(14), 4156–4157, DOI: 10.1021/JA0706504.
51 X. Liu, Y. Wang, P. Chen, A. McCadden, A. Palaniappan, J. Zhang and B. Liedberg, Peptide Functionalized Gold Nanoparticles with Optimized Particle Size and Concentration for Colorimetric Assay Development: Detection of Cardiac Troponin I, *ACS Sens.*, 2016, **1**(12), 1416–1422, DOI: 10.1021/acssensors.6b00493.
52 P. Englebienne, Use of Colloidal Gold Surface Plasmon Resonance Peak Shift to Infer Affinity Constants from the Interactions between Protein Antigens and Antibodies Specific for Single or Multiple Epitopes, *Analyst*, 1998, **123**(7), 1599–1603.
53 M. Anzevino, D. Marra, A. Fulgione, A. Giarra, D. Nava, L. Biondi, F. Capuano, V. Iannotti, B. Della Ventura and R. Velotta, Antibody-Functionalized Gold Nanoparticles as a Highly Sensitive Two-Step Colorimetric Biosensor for Detecting Salmonella Typhimurium in Food, *ACS Appl. Nano Mater.*, 2024, **7**(17), 21048–21056, DOI: 10.1021/acsanm.4c04134.
54 H. Tabassum, A. Maity, K. Singh, D. Bagchi, P. Nath, N. Kumar, S. Choudhury, S. Vishwakarma and A. Chakraborty, Elucidating Antibody Conjugation and Orientation Dynamics on Phenylalanine-Functionalized Gold Nanoparticles: The Role of Lipid Coating and Other Physiological Conditions, *Langmuir*, 2025, **41**(21), 12967–12980, DOI: 10.1021/acs.langmuir.5c00426.
55 R. Elghanian, J. J. Storhoff, R. C. Mucic, R. L. Letsinger and C. A. Mirkin, Selective Colorimetric Detection of Polynucleotides Based on the Distance-Dependent Optical Properties of Gold Nanoparticles, *Science*, 1997, **277**(5329), 1078–1081, DOI: 10.1126/SCIENCE.277.5329.1078.
56 N. Fukuzumi, G. Hirao, A. Ogawa, T. Asahi, M. Maeda and T. Zako, Density and Structure of DNA Immobilised on Gold Nanoparticles Affect Sensitivity in Nucleic Acid Detection, *Sci. Rep.*, 2025, **15**(1), 8222, DOI: 10.1038/s41598-025-92474-y.
57 M. M. Crane, *Organon MV. Diagnostic Test Device*, US3579306A, 1969.
58 I. J. Ezennia, S. O. Nduka and O. I. Ekwunife, Cost Benefit Analysis of Malaria Rapid Diagnostic Test: The Perspective of Nigerian Community Pharmacists, *Malar. J.*, 2017, **16**(1), 7–16, DOI: 10.1186/s12936-016-1648-0.
59 T. Tawiah, K. S. Hansen, F. Baiden, J. Bruce, M. Tivura, R. Delimini, S. Amengo-Etego, D. Chandramohan, S. Owusu-Agyei and J. Webster, Cost-Effectiveness Analysis of Test-Based *versus* Presumptive Treatment of Uncomplicated Malaria in Children under Five Years in an Area of High Transmission in Central Ghana, *PLoS One*, 2016, **11**(10), e0164055, DOI: 10.1371/journal.pone.0164055.
60 C. Aerts, M. Vink, S. J. Pashtoon, S. Nahzat, A. Picado, I. Cruz and E. Sicuri, Cost Effectiveness of New Diagnostic Tools for Cutaneous Leishmaniasis in Afghanistan, *Applied Health Economics and Health Policy*, 2019, vol. 17 (2), pp. 213–230, DOI: 10.1007/S40258-018-0449-8/TABLES/5.
61 J. C. Phan, J. Pettitt, J. S. George, L. S. Fakoli, F. M. Taweh, S. L. Bateman, R. S. Bennett, S. L. Norris, D. A. Spinnler, G. Pimentel, P. K. Sahr, F. K. Bolay and R. J. Schoepp, Lateral Flow Immunoassays for Ebola Virus Disease Detection in Liberia, *J. Infect. Dis.*, 2016, **214**(suppl 3), S222–S228, DOI: 10.1093/infdis/jiw251.
62 X. Mao, Y. Ma, A. Zhang, L. Zhang, L. Zeng and G. Liu, Disposable Nucleic Acid Biosensors Based on Gold Nanoparticle Probes and Lateral Flow Strip, *Anal. Chem.*, 2009, **81**(4), 1660–1668, DOI: 10.1021/ac8024653.
63 P. Damborský, K. M. Koczula, A. Gallotta and J. Katrlík, Lectin-Based Lateral Flow Assay: Proof-of-Concept, *Analyst*, 2016, **141**(23), 6444–6448, DOI: 10.1039/C6AN01746K.
64 A. S. John and C. P. Price, Existing and Emerging Technologies for Point-of-Care Testing, *Clin. Biochem. Rev.*, 2014, **35**(3), 155.
65 M. Müller, P. M. Derlet, C. Mudry and G. Aeppli, Testing of Asymptomatic Individuals for Fast Feedback-Control of COVID-19 Pandemic, *Phys. Biol.*, 2020, **17**(6), 065007, DOI: 10.1088/1478-3975/ABA6D0.
66 S. M. Moghadas, M. C. Fitzpatrick, P. Sah, A. Pandey, A. Shoukat, B. H. Singer and A. P. Galvani, The Implications of Silent Transmission for the Control of COVID-19 Outbreaks, *Proc. Natl. Acad. Sci. U. S. A.*, 2020, **117**(30), 17513–17515, DOI: 10.1073/pnas.2008373117/asset/2da5f309-3df6-45df-89af-31db75e11f7e/assets/images/large/pnas.2008373117fig01.jpg.
67 J. Ferguson, S. Dunn, A. Best, J. Mirza, B. Percival, M. Mayhew, O. Megram, F. Ashford, T. White, E. Moles-Garcia, L. Crawford, T. Plant, A. Bosworth, M. Kidd, A. Richter, J. Deeks and A. McNally, Validation Testing to Determine the Sensitivity of Lateral Flow Testing for Asymptomatic SARS-CoV-2 Detection in Low Prevalence Settings: Testing Frequency and Public Health Messaging Is Key, *PLoS Biol.*, 2021, **19**(4), e3001216, DOI: 10.1371/journal.pbio.3001216.
68 Z. Li, Y. Yi, X. Luo, N. Xiong, Y. Liu, S. Li, R. Sun, Y. Wang, B. Hu, W. Chen, Y. Zhang, J. Wang, B. Huang, Y. Lin, J. Yang, W. Cai, X. Wang, J. Cheng, Z. Chen, K. Sun, W. Pan, Z. Zhan, L. Chen and F. Ye, Development and Clinical Application of a Rapid IgM-IgG Combined Antibody Test for SARS-CoV-2 Infection Diagnosis, *J. Med. Virol.*, 2020, **92**(9), 1518–1524, DOI: 10.1002/JMV.25727.
69 T. Wen, C. Huang, F. J. Shi, X. Y. Zeng, T. Lu, S. N. Ding and Y. J. Jiao, Development of a Lateral Flow Immunoassay Strip for Rapid Detection of IgG Antibody against SARS-CoV-2 Virus, *Analyst*, 2020, **145**(15), 5345–5352, DOI: 10.1039/D0AN00629G.
70 Y. Liu, Y. P. Liu, B. Diao, J. Y. Ding, M. X. Yuan, F. F. Ren, Y. Wang, Q. C. Huang and P. F. Wei, Diagnostic Indexes of a Rapid Immunoglobulin G/Immunoglobulin M Combined Antibody Test for Severe Acute Respiratory Syndrome Coronavirus 2, *Chin. Med. J.*, 2021, **134**(4), 475–477, DOI: 10.1097/CM9.0000000000001204.
71 Assessment and procurement of coronavirus (COVID-19) tests - GOV.UK, https://www.gov.uk/government/publications/assessment-and-procurement-of-coronavirus-covid-19-tests#test-1-sd-biosensor-lateral-flow-test (accessed 2022-07-15).
72 Global partnership to make available 120 million affordable, quality COVID-19 rapid tests for low- and middle-income countries, https://www.who.int/news/item/28-09-2020-global-partnership-to-make-available-120-million-affordable-quality-covid-19-rapid-tests-for-low--and-middle-income-countries (accessed 2022-07-15).
73 S. Watanabe, H. Seguchi, K. Yoshida, K. Kifune, T. Tadaki and H. Shiozaki, Colorimetric Detection of Fluoride Ion in an Aqueous Solution Using a Thioglucose-Capped Gold Nanoparticle, *Tetrahedron Lett.*, 2005, **46**(51), 8827–8829, DOI: 10.1016/j.tetlet.2005.10.097.
74 S.-J. Richards, E. Fullam, G. S. Besra and M. I. Gibson, Discrimination between Bacterial Phenotypes Using Glyco-Nanoparticles and the Impact of Polymer Coating on Detection Readouts, *J. Mater. Chem. B*, 2014, **2**(11), 1490–1498, DOI: 10.1039/C3TB21821J.
75 C. L. Schofield, B. Mukhopadhyay, S. M. Hardy, M. B. McDonnell, R. A. Field and D. A. Russell, Colorimetric Detection ofRicinus Communis Agglutinin 120 Using Optimally Presented Carbohydrate-Stabilised Gold Nanoparticles, *Analyst*, 2008, **133**(5), 626–634, DOI: 10.1039/B715250G.
76 M. J. Marín, A. Rashid, M. Rejzek, S. A. Fairhurst, S. A. Wharton, S. R. Martin, J. W. McCauley, T. Wileman, R. A. Field and D. A. Russell, Glyconanoparticles for the Plasmonic Detection and Discrimination between Human and Avian Influenza Virus, *Org. Biomol. Chem.*, 2013, **11**(41), 7101–7107, DOI: 10.1039/C3OB41703D.
77 C. L. Schofield, M. J. Marín, M. Rejzek, P. R. Crocker, R. A. Field and D. A. Russell, Detection of mSiglec-E, in Solution and Expressed on the Surface of Chinese Hamster Ovary Cells, Using Sialic Acid Functionalised Gold Nanoparticles, *Analyst*, 2016, **141**(20), 5799–5809, DOI: 10.1039/C6AN01230B.
78 M. Takara, M. Toyoshima, H. Seto, Y. Hoshino and Y. Miura, Polymer-Modified Gold Nanoparticles via RAFT Polymerization: A Detailed Study for a Biosensing Application, *Polym. Chem.*, 2014, **5**(3), 931–939, DOI: 10.1039/c3py01001e.
79 J. Ishii, M. Toyoshima, M. Chikae, Y. Takamura and Y. Miura, Preparation of Glycopolymer-Modified Gold Nanoparticles and a New Approach for a Lateral Flow Assay, *Bull. Chem. Soc. Jpn.*, 2011, **84**(5), 466–470, DOI: 10.1246/bcsj.20100303.
80 A. L. Parry, N. A. Clemson, J. Ellis, S. S. R. Bernhard, B. G. Davis and N. R. Cameron, ''Multicopy Multivalent'' Glycopolymer-Stabilized Gold Nanoparticles as Potential Synthetic Cancer Vaccines, *J. Am. Chem. Soc.*, 2013, **135**(25), 9362–9365, DOI: 10.1021/ja4046857.

81 S. Perrier, 50th Anniversary Perspective: RAFT Polymerization—A User Guide, *Macromolecules*, 2017, **50**(19), 7433–7447, DOI: 10.1021/acs.macromol.7b00767.
82 S.-J. Richards and M. I. Gibson, Optimization of the Polymer Coating for Glycosylated Gold Nanoparticle Biosensors to Ensure Stability and Rapid Optical Readouts, *ACS Macro Lett.*, 2014, **3**(10), 1004–1008, DOI: 10.1021/mz5004882.
83 N. S. Ieong, C. I. Biggs, M. Walker and M. I. Gibson, Comparison of RAFT Derived Poly(Vinylpyrolidone) Verses Poly(Oligoethyleneglycol Methacrylate) for the Stabilization of Glycosylated Gold Nanoparticles, *J. Polym. Sci., Part A: Polym. Chem.*, 2017, **55**(7), 1200–1208, DOI: 10.1002/pola.28481.
84 N. S. Ieong, K. Brebis, L. E. Daniel, R. K. O'Reilly and M. I. Gibson, The Critical Importance of Size on Thermoresponsive Nanoparticle Transition Temperatures: Gold and Micelle-Based Polymer Nanoparticles, *Chem. Commun.*, 2011, **47**(42), 11627–11629, DOI: 10.1039/C1CC15171A.
85 P. J. Roth, D. Kessler, R. Zentel and P. Theato, Versatile ω-End Group Functionalization of RAFT Polymers Using Functional Methane Thiosulfonates, *J. Polym. Sci., Part A: Polym. Chem.*, 2009, **47**(12), 3118–3130, DOI: 10.1002/pola.23392.
86 S.-J. Richards, A. N. Baker, M. Walker and M. I. Gibson, Polymer-Stabilized Sialylated Nanoparticles: Synthesis, Optimization, and Differential Binding to Influenza Hemagglutinins, *Biomacromolecules*, 2020, **21**(4), 1604–1612, DOI: 10.1021/acs.biomac.0c00179.
87 J. Micallef, A. N. Baker, S.-J. Richards, D. E. Soutar, P. G. Georgiou, M. Walker and M. I. Gibson, Polymer-Tethered Glyconanoparticle Colourimetric Biosensors for Lectin Binding: Structural and Experimental Parameters to Ensure a Robust Output, *RSC Adv.*, 2022, **12**(51), 33080–33090, DOI: 10.1039/D2RA06265H.
88 T. R. Branson and W. B. Turnbull, Bacterial Toxin Inhibitors Based on Multivalent Scaffolds, *Chem. Soc. Rev.*, 2013, **42**(11), 4613–4622, DOI: 10.1039/c2cs35430f.
89 Y. Abdouni, G. Yilmaz and C. R. Becer, Sequence and Architectural Control in Glycopolymer Synthesis, *Macromol. Rapid Commun.*, 2017, **38**(24), 1700212, DOI: 10.1002/marc.201700212.
90 S.-J. Richards, M. W. Jones, M. Hunaban, D. M. Haddleton and M. I. Gibson, Probing Bacterial-Toxin Inhibition with Synthetic Glycopolymers Prepared by Tandem Post-Polymerization Modification: Role of Linker Length and Carbohydrate Density, *Angew. Chem., Int. Ed.*, 2012, **51**(31), 7812–7816, DOI: 10.1002/anie.201202945.
91 B. D. Polizzotti and K. L. Kiick, Effects of Polymer Structure on the Inhibition of Cholera Toxin by Linear Polypeptide-Based Glycopolymers, *Biomacromolecules*, 2006, **7**(2), 483–490, DOI: 10.1021/bm050672n.
92 C. M. Jarvis, D. B. Zwick, J. C. Grim, M. M. Alam, L. R. Prost, J. C. Gardiner, S. Park, L. L. Zimdars, N. M. Sherer and L. L. Kiessling, Antigen Structure Affects Cellular Routing through DC-SIGN, *Proc. Natl. Acad. Sci. U. S. A.*, 2019, **116**(30), 14862–14867, DOI: 10.1073/pnas.1820165116.
93 P. G. Georgiou, A. N. Baker, S. J. Richards, A. Laezza, M. Walker and M. I. Gibson, Tuning Aggregative *versus* Non-Aggregative Lectin Binding with Glycosylated Nanoparticles by the Nature of the Polymer Ligand, *J. Mater. Chem. B*, 2020, **8**(1), 136–145, DOI: 10.1039/C9TB02004G.
94 M. Ambrosi, A. S. Batsanov, N. R. Cameron, B. G. Davis, J. A. K. Howard and R. Hunter, Influence of Preparation Procedure on Polymer Composition: Synthesis and Characterisation of Polymethacrylates Bearing β-D-Glucopyranoside and β-D-Galactopyranoside Residues, *J. Chem. Soc., Perkin Trans. 1*, 2002, 45–52, DOI: 10.1039/B108421F.
95 M. A. Gauthier, M. I. Gibson and H.-A. Klok, Synthesis of Functional Polymers by Post-Polymerization Modification, *Angew. Chem., Int. Ed.*, 2009, **48**(1), 48–58, DOI: 10.1002/anie.200801951.
96 V. Ladmiral, G. Mantovani, G. J. Clarkson, S. Cauet, J. L. Irwin and D. M. Haddleton, Synthesis of Neoglycopolymers by a Combination of "Click Chemistry" and Living Radical Polymerization, *J. Am. Chem. Soc.*, 2006, **128**(14), 4823–4830, DOI: 10.1021/ja058364k.
97 G. Chen, S. Amajjahe and M. H. Stenzel, Synthesis of Thiol-Linked Neoglycopolymers and Thermo-Responsive Glycomicelles as Potential Drug Carrier, *Chem. Commun.*, 2009, 1198–1200, DOI: 10.1039/B900215D.
98 M. Semsarilar, V. Ladmiral and S. Perrier, Highly Branched and Hyperbranched Glycopolymers via Reversible Addition−Fragmentation Chain Transfer Polymerization and Click Chemistry, *Macromolecules*, 2010, **43**(3), 1438–1443, DOI: 10.1021/ma902587r.
99 C. Boyer, A. Bousquet, J. Rondolo, M. R. Whittaker, M. H. Stenzel and T. P. Davis, Glycopolymer Decoration of Gold Nanoparticles Using a LbL Approach, *Macromolecules*, 2010, **43**(8), 3775–3784, DOI: 10.1021/ma100250x.
100 M. I. Gibson, E. Fröhlich and H.-A. Klok, Postpolymerization Modification of Poly(Pentafluorophenyl Methacrylate): Synthesis of a Diverse Water-Soluble Polymer Library, *J. Polym. Sci., Part A: Polym. Chem.*, 2009, **47**(17), 4332–4345, DOI: 10.1002/pola.23486.
101 M. W. Jones, S.-J. Richards, D. M. Haddleton and M. I. Gibson, Poly(Azlactone)s: Versatile Scaffolds for Tandem Post-Polymerisation Modification and Glycopolymer Synthesis, *Polym. Chem.*, 2013, **4**(3), 717–723, DOI: 10.1039/C2PY20757E.
102 L. E. Wilkins, N. Badi, F. Du Prez and M. I. Gibson, Double-Modified Glycopolymers from Thiolactones to Modulate Lectin Selectivity and Affinity, *ACS Macro Lett.*, 2018, **7**(12), 1498–1502, DOI: 10.1021/acsmacrolett.8b00825.
103 T. Tanaka, H. Nagai, M. Noguchi, A. Kobayashi and S. Shoda, One-Step Conversion of Unprotected Sugars to β-Glycosyl Azides Using 2-Chloroimidazolinium Salt in Aqueous Solution, *Chem. Commun.*, 2009, 3378–3379, DOI: 10.1039/B905761G.
104 D. Lim, M. A. Brimble, R. Kowalczyk, A. J. A. Watson and A. J. Fairbanks, Protecting-Group-Free One-Pot Synthesis of Glycoconjugates Directly from Reducing Sugars, *Angew. Chem., Int. Ed.*, 2014, **53**(44), 11907–11911, DOI: 10.1002/anie.201406694.
105 K. Godula and C. R. Bertozzi, Synthesis of Glycopolymers for Microarray Applications via Ligation of Reducing Sugars to a Poly(Acryloyl Hydrazide) Scaffold, *J. Am. Chem. Soc.*, 2010, **132**(29), 9963–9965, DOI: 10.1021/ja103009d.
106 S.-J. Richards, L. Otten and M. I. Gibson, Glycosylated Gold Nanoparticle Libraries for Label-Free Multiplexed Lectin Biosensing, *J. Mater. Chem. B*, 2016, **4**(18), 3046–3053, DOI: 10.1039/C5TB01994J.
107 D. N. Crisan, O. Creese, R. Ball, J. L. Brioso, B. Martyn, J. Montenegro and F. Fernandez-Trillo, Poly(Acryloyl Hydrazide), a Versatile Scaffold for the Preparation of Functional Polymers: Synthesis and Post-Polymerisation Modification, *Polym. Chem.*, 2017, **8**(31), 4576–4584, DOI: 10.1039/C7PY00535K.
108 C. S. Mahon, M. A. Fascione, C. Sakonsinsiri, T. E. McAllister, W. B. Turnbull and D. A. Fulton, Templating Carbohydrate-Functionalised Polymer-Scaffolded Dynamic Combinatorial Libraries with Lectins, *Org. Biomol. Chem.*, 2015, **13**(9), 2756–2761, DOI: 10.1039/C4OB02587C.
109 J. Kalia and R. T. Raines, Hydrolytic Stability of Hydrazones and Oximes, *Angew. Chem., Int. Ed.*, 2008, **47**(39), 7523–7526, DOI: 10.1002/anie.200802651.
110 C. Pifferi, G. C. Daskhan, M. Fiore, T. C. Shiao, R. Roy and O. Renaudet, Aminooxylated Carbohydrates: Synthesis and Applications, *Chem. Rev.*, 2017, **117**(15), 9839–9873, DOI: 10.1021/acs.chemrev.6b00733.
111 A. Laezza, P. G. Georgiou, S.-J. Richards, A. N. Baker, M. Walker and M. I. Gibson, Protecting Group Free Synthesis of Glyconanoparticles Using Amino–Oxy-Terminated Polymer Ligands, *Bioconjugate Chem.*, 2020, **31**(10), 2392–2403, DOI: 10.1021/acs.bioconjchem.0c00465.
112 X. Wang, O. Ramström and M. Yan, A Photochemically Initiated Chemistry for Coupling Underivatized Carbohydrates to Gold Nanoparticles, *J. Mater. Chem.*, 2009, **19**(47), 8944–8949, DOI: 10.1039/B917900C.
113 X. Wang, O. Ramström and M. Yan, Quantitative Analysis of Multivalent Ligand Presentation on Gold Glyconanoparticles and the Impact on Lectin Binding, *Anal. Chem.*, 2010, **82**(21), 9082–9089, DOI: 10.1021/ac102114z.
114 H. S. N. Jayawardena, X. Wang and M. Yan, Classification of Lectins by Pattern Recognition Using Glyconanoparticles, *Anal. Chem.*, 2013, **85**(21), 10277–10281, DOI: 10.1021/ac402069j.
115 L. Otten, D. Vlachou, S.-J. Richards and M. I. Gibson, Glycan Heterogeneity on Gold Nanoparticles Increases Lectin Discrimination Capacity in Label-Free Multiplexed Bioassays, *Analyst*, 2016, **141**(14), 4305–4312, DOI: 10.1039/C6AN00549G.
116 S. Won, S.-J. Richards, M. Walker and M. I. Gibson, Externally Controllable Glycan Presentation on Nanoparticle Surfaces to Modulate Lectin Recognition, *Nanoscale Horiz.*, 2017, **2**(2), 106–109, DOI: 10.1039/C6NH00202A.

117 A. N. Baker, S.-J. Richards, C. S. Guy, T. R. Congdon, M. Hasan, A. J. Zwetsloot, A. Gallo, J. R. Lewandowski, P. J. Stansfeld, A. Straube, M. Walker, S. Chessa, G. Pergolizzi, S. Dedola, R. A. Field and M. I. Gibson, The SARS-COV-2 Spike Protein Binds Sialic Acids and Enables Rapid Detection in a Lateral Flow Point of Care Diagnostic Device, *ACS Cent. Sci.*, 2020, **6**(11), 2046–2052, DOI: 10.1021/acscentsci.0c00855.

118 A. N. Baker, S.-J. Richards, S. Pandey, C. S. Guy, A. Ahmad, M. Hasan, C. I. Biggs, P. G. Georgiou, A. J. Zwetsloot, A. Straube, S. Dedola, R. A. Field, N. R. Anderson, M. Walker, D. Grammatopoulos and M. I. Gibson, Glycan-Based Flow-Through Device for the Detection of SARS-COV-2, *ACS Sens.*, 2021, **6**(10), 3696–3705, DOI: 10.1021/acssensors.1c01470.

119 A. N. Baker, A. R. Muguruza, S.-J. Richards, P. G. Georgiou, S. Goetz, M. Walker, S. Dedola, R. A. Field and M. I. Gibson, Lateral Flow Glyco-Assays for the Rapid and Low-Cost Detection of Lectins–Polymeric Linkers and Particle Engineering Are Essential for Selectivity and Performance, *Adv. Healthcare Mater.*, 2022, **11**(4), 2101784, DOI: 10.1002/adhm.202101784.

120 A. Ahmad, P. G. Georgiou, A. Pancaro, M. Hasan, I. Nelissen and M. I. Gibson, Polymer-Tethered Glycosylated Gold Nanoparticles Recruit Sialylated Glycoproteins into Their Protein Corona, Leading to off-Target Lectin Binding, *Nanoscale*, 2022, **14**(36), 13261–13273, DOI: 10.1039/D2NR01818G.

121 P. G. Georgiou, C. S. Guy, M. Hasan, A. Ahmad, S.-J. Richards, A. N. Baker, N. V. Thakkar, M. Walker, S. Pandey, N. R. Anderson, D. Grammatopoulos and M. I. Gibson, Plasmonic Detection of SARS-CoV-2 Spike Protein with Polymer-Stabilized Glycosylated Gold Nanorods, *ACS Macro Lett.*, 2022, **11**(3), 317–322, DOI: 10.1021/acsmacrolett.1c00716.

122 M. Eberhardt, R. Mruk, R. Zentel and P. Théato, Synthesis of Pentafluorophenyl(Meth)Acrylate Polymers: New Precursor Polymers for the Synthesis of Multifunctional Materials, *Eur. Polym. J.*, 2005, **41**(7), 1569–1575, DOI: 10.1016/j.eurpolymj.2005.01.025.

123 M. Eberhardt and P. Théato, RAFT Polymerization of Pentafluorophenyl Methacrylate: Preparation of Reactive Linear Diblock Copolymers, *Macromol. Rapid Commun.*, 2005, **26**(18), 1488–1493, DOI: 10.1002/marc.200500390.

124 S.-J. Richards, M. W. Jones, M. Hunaban, D. M. Haddleton and M. I. Gibson, Probing Bacterial-Toxin Inhibition with Synthetic Glycopolymers Prepared by Tandem Post-Polymerization Modification: Role of Linker Length and Carbohydrate Density, *Angew. Chem., Int. Ed.*, 2012, **51**(31), 7812–7816, DOI: 10.1002/anie.201202945.

125 B. Martyn, C. I. Biggs and M. I. Gibson, Comparison of Systematically Functionalized Heterogeneous and Homogenous Glycopolymers as Toxin Inhibitors, *J. Polym. Sci., Part A: Polym. Chem.*, 2019, **57**(1), 40–47, DOI: 10.1002/pola.29279.

126 N. J. Agard, J. A. Prescher and C. R. Bertozzi, A Strain-Promoted [3 + 2] Azide–Alkyne Cycloaddition for Covalent Modification of Biomolecules in Living Systems, *J. Am. Chem. Soc.*, 2004, **126**(46), 15046–15047, DOI: 10.1021/ja044996f.

127 S.-J. Richards, S. Chessa, L. Sayer, I. Ivanova, S. Ahmadipour, A. N. Baker, M. Walker, S. Dedola, K. A. Scott, O. Dibben, R. A. Field and M. I. Gibson, Label-Free and Microplate-Based Dissection of Glycan-Virus Interactions Using Polymer-Tethered Glyconanoparticles, *Small Methods*, 2025, e2500214, DOI: 10.1002/smtd.202500214.

128 S.-J. Richards, T. Keenan, J.-B. Vendeville, D. E. Wheatley, H. Chidwick, D. Budhadev, C. E. Council, C. S. Webster, H. Ledru, A. N. Baker, M. Walker, M. C. Galan, B. Linclau, M. A. Fascione and M. I. Gibson, Introducing Affinity and Selectivity into Galectin-Targeting Nanoparticles with Fluorinated Glycan Ligands, *Chem. Sci.*, 2021, **12**(3), 905–910, DOI: 10.1039/D0SC05360K.

129 K. Hollingsworth, A. Di Maio, S.-J. Richards, J.-B. Vendeville, D. E. Wheatley, C. E. Council, T. Keenan, H. Ledru, H. Chidwick, K. Huang, F. Parmeggiani, A. Marchesi, W. Chai, R. McBerney, T. P. Kamiński, M. R. Balmforth, A. Tamasanu, J. D. Finnigan, C. Young, S. L. Warriner, M. E. Webb, M. A. Fascione, S. Flitsch, M. C. Galan, T. Feizi, M. I. Gibson, Y. Liu, W. B. Turnbull and B. Linclau, Synthesis and Screening of a Library of Lewisx Deoxyfluoro-Analogues Reveals Differential Recognition by Glycan-Binding Partners, *Nat. Commun.*, 2024, **15**(1), 7925, DOI: 10.1038/s41467-024-51081-7.

130 D. Budhadev, E. Poole, I. Nehlmeier, Y. Liu, J. Hooper, E. Kalverda, U. S. Akshath, N. Hondow, W. B. Turnbull, S. Pöhlmann, Y. Guo and D. Zhou, Glycan-Gold Nanoparticles as Multifunctional Probes for Multivalent Lectin–Carbohydrate Binding: Implications for Blocking Virus Infection and Nanoparticle Assembly, *J. Am. Chem. Soc.*, 2020, **142**(42), 18022–18034, DOI: 10.1021/jacs.0c06793.

131 A. L. Parry, N. A. Clemson, J. Ellis, S. S. R. Bernhard, B. G. Davis and N. R. Cameron, 'Multicopy Multivalent' Glycopolymer-Stabilized Gold Nanoparticles as Potential Synthetic Cancer Vaccines, *J. Am. Chem. Soc.*, 2013, **135**(25), 9362–9365, DOI: 10.1021/ja4046857.

132 A. M. Smith, L. E. Marbella, K. A. Johnston, M. J. Hartmann, S. E. Crawford, L. M. Kozycz, D. S. Seferos and J. E. Millstone, Quantitative Analysis of Thiolated Ligand Exchange on Gold Nanoparticles Monitored by 1H NMR Spectroscopy, *Anal. Chem.*, 2015, **87**(5), 2771–2778, DOI: 10.1021/ac504081k.

133 S. Nicolardi, Y. E. M. van der Burgt, J. D. C. Codée, M. Wuhrer, C. H. Hokke and F. Chiodo, Structural Characterization of Biofunctionalized Gold Nanoparticles by Ultrahigh-Resolution Mass Spectrometry, *ACS Nano*, 2017, **11**(8), 8257–8264, DOI: 10.1021/acsnano.7b03402.

134 E. Scott, E. Archer Goode, R. Garnham, K. Hodgson, M. Orozco-Moreno, H. Turner, K. Livermore, K. Putri Nangkana, F. M. Frame, A. Bermudez, F. Jose Garcia Marques, U. L. McClurg, L. Wilson, H. Thomas, A. Buskin, A. Hepburn, A. Duxfield, K. Bastian, H. Pye, H. M. Arredondo, G. Hysenaj, S. Heavey, U. Stopka-Farooqui, A. Haider, A. Freeman, S. Singh, E. W. Johnston, S. Punwani, B. Knight, P. McCullagh, J. McGrath, M. Crundwell, L. Harries, R. Heer, N. J. Maitland, H. Whitaker, S. Pitteri, D. A. Troyer, N. Wang, D. J. Elliott, R. R. Drake and J. Munkley, ST6GAL1 -mediated Aberrant Sialylation Promotes Prostate Cancer Progression, *J. Pathol.*, 2023, **261**(1), 71–84, DOI: 10.1002/path.6152.

135 T. Feizi, F. Fazio, W. Chai and C. H. Wong, Carbohydrate Microarrays - a New Set of Technologies at the Frontiers of Glycomics, *Curr. Opin. Struct. Biol.*, 2003, **13**(5), 637–645.

136 W. B. Turnbull, B. L. Precious and S. W. Homans, Dissecting the Cholera Toxin-Ganglioside GM1 Interaction by Isothermal Titration Calorimetry, *J. Am. Chem. Soc.*, 2004, **126**(4), 1047–1054, DOI: 10.1021/ja0378207.

137 M. Toyoshima and Y. Miura, Preparation of Glycopolymer-Substituted Gold Nanoparticles and Their Molecular Recognition, *J. Polym. Sci., Part A: Polym. Chem.*, 2009, **47**(5), 1412–1421, DOI: 10.1002/pola.23250.

138 K. G. Leslie, K. A. Jolliffe, M. Müllner, E. J. New, W. B. Turnbull, M. A. Fascione, V.-P. Friman and C. S. Mahon, A Glycopolymer Sensor Array That Differentiates Lectins and Bacteria, *Biomacromolecules*, 2024, **25**(11), 7466–7474, DOI: 10.1021/acs.biomac.4c01129.

139 R. A. Childs, A. S. Palma, S. Wharton, T. Matrosovich, Y. Liu, W. Chai, M. A. Campanero-Rhodes, Y. Zhang, M. Eickmann, M. Kiso, A. Hay, M. Matrosovich and T. Feizi, Receptor-Binding Specificity of Pandemic Influenza A (H1N1) 2009 Virus Determined by Carbohydrate Microarray, *Nat. Biotechnol.*, 2009, **27**(9), 797–799, DOI: 10.1038/nbt0909-797.

140 A. Canales, J. Sastre, J. M. Orduña, C. M. Spruit, J. Pérez-Castells, G. Domínguez, K. M. Bouwman, R. van der Woude, F. J. Cañada, C. M. Nycholat, J. C. Paulson, G.-J. Boons, J. Jiménez-Barbero and R. P. de Vries, Revealing the Specificity of Human H1 Influenza A Viruses to Complex N -Glycans, *JACS Au*, 2023, **3**(3), 868–878, DOI: 10.1021/jacsau.2c00664.

141 L. Nguyen, K. A. McCord, D. T. Bui, K. M. Bouwman, E. N. Kitova, M. Elaish, D. Kumawat, G. C. Daskhan, I. Tomris, L. Han, P. Chopra, T.-J. Yang, S. D. Willows, A. L. Mason, L. K. Mahal, T. L. Lowary, L. J. West, S.-T. D. Hsu, T. Hobman, S. M. Tompkins, G.-J. Boons, R. P. de Vries, M. S. Macauley and J. S. Klassen, Sialic Acid-Containing Glycolipids Mediate Binding and Viral Entry of SARS-CoV-2, *Nat. Chem. Biol.*, 2022, **18**(1), 81–90, DOI: 10.1038/s41589-021-00924-1.

142 C. J. Buchanan, B. Gaunt, P. J. Harrison, Y. Yang, J. Liu, A. Khan, A. M. Giltrap, A. Le Bas, P. N. Ward, K. Gupta, M. Dumoux, T. K. Tan, L. Schimaski, S. Daga, N. Picchiotti, M. Baldassarri, E. Benetti, C. Fallerini, F. Fava, A. Giliberti, P. I. Koukos, M. J. Davy, A. Lakshminarayanan, X. Xue, G. Papadakis, L. P. Deimel, V. Casablancas-Antràs, T. D. W. Claridge, A. M. J. J. Bonvin, Q. J. Sattentau, S. Furini, M. Gori, J. Huo, R. J. Owens, C. Schaffitzel, I. Berger, A. Renieri, J. H. Naismith, A. J. Baldwin,

B. G. Davis and B. G. Davis, Pathogen-Sugar Interactions Revealed by Universal Saturation Transfer Analysis, *Science*, 2022, **377**, 6604, DOI: 10.1126/science.abm3125.

143 S. J. L. Petitjean, W. Chen, M. Koehler, R. Jimmidi, J. Yang, D. Mohammed, B. Juniku, M. L. Stanifer, S. Boulant, S. P. Vincent and D. Alsteens, Multivalent 9-O-Acetylated-Sialic Acid Glycoclusters as Potent Inhibitors for SARS-CoV-2 Infection, *Nat. Commun.*, 2022, **13**(1), 2564, DOI: 10.1038/s41467-022-30313-8.

144 M. A. Sparks, K. W. Williams and G. M. Whitesides, Neuraminidase-Resistant Hemagglutination Inhibitors: Acrylamide Copolymers Containing a C-Glycoside of N-Acetylneuraminic Acid, *J. Med. Chem.*, 1993, **36**(6), 778–783, DOI: 10.1021/jm00058a016.

145 M. Brito-Arias, C-Glycosides. *In Synthesis and Characterization of Glycosides*, ed M. Brito-Arias, Springer International Publishing, Cham, 2022, pp. 367–402, DOI: 10.1007/978-3-030-97854-9_5.

146 A. N. Baker, G. W. Hawker-Bond, P. G. Georgiou, S. Dedola, R. A. Field and M. I. Gibson, Glycosylated Gold Nanoparticles in Point of Care Diagnostics: From Aggregation to Lateral Flow, *Chem. Soc. Rev.*, 2022, **51**(16), 7238–7259, DOI: 10.1039/D2CS00267A.

147 P. Damborský, K. M. Koczula, A. Gallotta and J. Katrlík, Lectin-Based Lateral Flow Assay: Proof-of-Concept, *Analyst*, 2016, **141**(23), 6444–6448, DOI: 10.1039/C6AN01746K.

148 P. J. Hernando, I. M. Ivanova, S. Chessa, M. J. Marín, S. Dedola and R. A. Field, Sensitive Dipstick Assays for Lectin Detection, Based on Glycan–BSA Conjugate Immobilisation on Gold Nanoparticles, *Org. Chem. Front.*, 2023, **10**(15), 3819–3829, DOI: 10.1039/D3QO00424D.

149 S. H. Kim, F. L. Kearns, M. A. Rosenfeld, L. Casalino, M. J. Papanikolas, C. Simmerling, R. E. Amaro and R. Freeman, GlycoGrip: Cell Surface-Inspired Universal Sensor for Betacoronaviruses, *ACS Cent. Sci.*, 2022, **8**(1), 22–42, DOI: 10.1021/acscentsci.1c01080.

150 A. N. Baker, T. R. Congdon, S.-J. Richards, P. G. Georgiou, M. Walker, S. Dedola, R. A. Field and M. I. Gibson, End-Functionalized Poly(Vinylpyrrolidone) for Ligand Display in Lateral Flow Device Test Lines, *ACS Polym. Au*, 2022, **2**(2), 69–79, DOI: 10.1021/acspolymersau.1c00032.

151 A. Ahmad, P. Georgiou, M. Hasan, A. Pancaro, I. Nelissen and M. I. Gibson, Polymer-Tethered Glycosylated Gold Nanoparticles Recruit Sialylated Glycoproteins into Their Protein Corona, Leading to Off-Target Lectin Binding, *Nanoscale*, 2022, **14**, 13261–13273, DOI: 10.1039/d2nr01818g.

152 S. Won, S.-J. Richards, M. Walker and M. I. Gibson, Externally Controllable Glycan Presentation on Nanoparticle Surfaces to Modulate Lectin Recognition, *Nanoscale Horiz.*, 2017, **3**(2), 1593–1608, DOI: 10.1039/C6NH00202A.